



Relationships between metabolic profiles and gene expression in liver and leukocytes of dairy cows in early lactation

D. C. Wathes,^{1*} Z. Cheng,¹ M. Salavati,^{1†} L. Buggiotti,¹ H. Takeda,² L. Tang,² F. Becker,³ K. I. Ingvarsen,⁴ C. Ferris,⁵ M. Hostens,⁶ M. A. Crowe,⁷ and the GplusE Consortium‡

¹Royal Veterinary College, Hatfield, AL9 7TA Hertfordshire, United Kingdom

²Unit of Animal Genomics, GIGA Institute, University of Liège, B-4000 Liège, Belgium

³Leibniz Institute for Farm Animal Biology, 18196 Dummerstorf, Germany

⁴Department of Animal Science, Aarhus University, DK-8830 Tjele, Denmark

⁵Agri-Food and Biosciences Institute, Belfast BT9 5PX, United Kingdom

⁶Department of Reproduction, Obstetrics and Herd Health, Ghent University, B-9820 Merelbeke, Belgium

⁷School of Veterinary Medicine, University College Dublin, Dublin 4, Ireland

ABSTRACT

Homeorhetic mechanisms assist dairy cows in the transition from pregnancy to lactation. Less successful cows develop severe negative energy balance (NEB), placing them at risk of metabolic and infectious diseases and reduced fertility. We have previously placed multiparous Holstein Friesian cows from 4 herds into metabolic clusters, using as biomarkers measurements of plasma nonesterified fatty acids, β -hydroxybutyrate, glucose and IGF-1 collected at 14 and 35 d in milk (DIM). This study characterized the global transcriptomic profiles of liver and circulating leukocytes from the same animals to determine underlying mechanisms associated with their metabolic and immune function.

Liver biopsy and whole-blood samples were collected around 14 DIM for RNA sequencing. All cows with available RNA sequencing data were placed into balanced (BAL, $n = 44$), intermediate ($n = 44$), or imbalanced (IMBAL, $n = 19$) metabolic cluster groups. Differential gene expression was compared between the 3 groups using ANOVA, but only the comparison between BAL and IMBAL cows is reported. Pathway analysis was undertaken using DAVID Bioinformatic Resources (<https://david.ncifcrf.gov/>). Milk yields did not differ between BAL and IMBAL cows but dry matter intake was less in IMBAL cows and they were in greater energy deficit at 14 DIM (-4.48 v -11.70 MJ/d for BAL and IMBAL cows). Significantly differentially expressed pathways in hepatic tissue included AMPK signaling, glucagon signaling, adipocytokine signaling, and insulin resistance. Genes involved in lipid metabolism and cholesterol transport were more highly expressed in IMBAL cows but *IGF1* and *IGFALS* were downregulated. Leukocytes from BAL cows had greater expression of histones and genes involved in nucleosomes and cell division. Leukocyte expression of heat shock proteins increased in IMBAL cows, suggesting an unfolded protein response, and several key genes involved in immune responses to pathogens were upregulated (e.g., *DEFB13*, *HP*, *OAS1Z*, *PTX3*, and *TLR4*). Differentially expressed genes upregulated in IMBAL cows in both tissues included *CD36*, *CPT1*, *KFL11*, and *PDK4*, all central regulators of energy metabolism. The IMBAL cows therefore had greater difficulty maintaining glucose homeostasis and had dysregulated hepatic lipid metabolism. Their energy deficit was associated with a reduced capacity for cell division and greater evidence of stress responses in the leukocyte population, likely contributing to an increased risk of infectious disease.

Key words: metabolic clustering, RNA sequencing, liver, leukocyte, negative energy balance

Received June 26, 2020.

Accepted October 11, 2020.

*Corresponding author: dcwathes@rvc.ac.uk

†Current address: The Roslin Institute, Royal (Dick) School of Veterinary Studies, Easter Bush Campus, Midlothian, United Kingdom.

‡Authors in the GplusE Consortium: Niamh McLoughlin, Alan Fahey, Elizabeth Matthews, Andrea Santoro, Colin Byrne, Pauline Rudd, Roisin O'Flaherty, Sinead Hallinan, Claire Wathes, Zhangrui Cheng, Ali Fouladi, Geoff Pollott, Dirk Werling, Beatriz Sanz Bernardo, Mazdak Salavati, Laura Buggiotti, Alistair Wylie, Matt Bell, Mieke Vaneetvelde, Kristof Hermans, Geert Opsomer, Sander Moerman, Jenne De Koster, Hannes Bogaert, Jan Vandepitte, Leila Vandavelde, Bonny Vanranst, Johanna Hoglund, Susanne Dahl, Soren Ostergaard, Janne Rothmann, Mogens Krogh, Else Meyer, Charlotte Gaillard, Jehan Ettema, Tine Rousing, Federica Signorelli, Francesco Napolitano, Bianca Moiola, Alessandra Crisa, Luca Buttazzoni, Jennifer McClure, Daragh Matthews, Francis Kearney, Andrew Cromie, Matt McClure, Shujun Zhang, Xing Chen, Huanchun Chen, Junlong Zhao, Liguang Yang, Guohua Hua, Chen Tan, Guiqiang Wang, Michel Bonneau, Andrea Pompozzi, Armin Pearn, Arnold Everson, Linda Kosten, Anders Fogh, Thomas Andersen, Matthew Lucy, Chris Elvik, Gavin Conant, Jerry Taylor, Nicolas Gengler, Michel Georges, Frederic Colinet, Marilou Ramos Pamplona, Hedi Hammami, Catherine Bastin, Haruko Takeda, Aurelie Laine, Anne-Sophie Van Laere, Martin Schulze, Cinzia Marchitelli, Frank Becker, and Sergio Palma Vera.

INTRODUCTION

Dairy cows undergo extensive metabolic and endocrine changes as they transition from pregnancy to lactation (Bell, 1995; Drackley et al., 2001; Chagas et al., 2007). Some of the metabolic and humoral signals affect appetite during the periparturient period, influenced by many individual cow factors, including health and age, together with management and environmental factors such as feed availability and temperature (Ingvarlsen and Andersen, 2000; Ingvarlsen, 2006). Cows have been selected to promote nutrient partitioning, and the associated endocrine shifts in transition cows cause major body tissue mobilization, which in turn reduces appetite and thus feed intake. When DMI fails to keep pace with the rising energy requirements of early lactation, cows enter a period of negative energy balance (**NEB**), which may last for several months in severe cases (Taylor et al., 2003). The liver coordinates the extensive metabolic changes required via upregulation of genes involved in fatty acid oxidation and gluconeogenesis and downregulation of triacylglycerol synthesis (Lor et al., 2006; Habel and Sundrum, 2020). These changes are reflected in circulating metabolite concentrations, with increased concentrations of nonesterified fatty acids (**NEFA**) and BHB and decreased concentrations of glucose. This may be associated with the development of hepatic steatosis (fatty liver disease; Vernon, 2005; Ingvarlsen, 2006; Shi et al., 2020).

Extensive changes to the somatotrophic axis also occur during the peripartum period. Growth hormone plays a key role in milk production by promoting lipolysis and gluconeogenesis (Bauman, 1999). The hepatic growth hormone (**GH**) receptor is, however, downregulated at this time (Lucy, 2008), causing a sharp decline in the synthesis of IGF-1. For cows in severe NEB, the hepatic expression of transcripts encoding IGF binding proteins (**IGFBP**)-3, -4, -5, and -6 and the acid labile subunit are also reduced, whereas expression of IGFBP-2 is elevated (Fenwick et al., 2008). These changes not only lead to a reduction in circulating IGF-1, but also reduce its half-life and bioavailability (Clemmons, 1997; Bach, 2018). As lactation progresses, the GH-IGF-1 axis becomes recoupled, so IGF-1 concentrations increase again (Wathes et al., 2007a; Lucy, 2008).

Some cows are less able than others to respond appropriately to the demands placed on them in early lactation. They then become metabolically imbalanced, placing them at increased risk of suffering from metabolic and infectious diseases (Ingvarlsen, 2006; Moyes et al., 2013; Habel and Sundrum, 2020). Cows with a low IGF-1 nadir in the first 2 wk after calving are also less likely to conceive (Taylor et al., 2004; Wathes et al., 2007a). Elevated NEFA and BHB and decreased

glucose and IGF-1 are thus recognized as biomarkers of an unsuccessful transition from the dry period to lactation (Ingvarlsen et al., 2003; Puppel and Kuczyńska, 2016). We recently demonstrated that a *k*-means clustering technique could be used to combine information based on the log-transformed and standardized concentrations of these 4 metabolic biomarkers in blood to identify individual cows with balanced or imbalanced metabolic profiles (De Koster et al., 2019). Samples were collected at around 14 DIM (early lactation) and 35 DIM (peak lactation) and data from both time points were considered in the classification. The study by De Koster et al. (2019) showed that the metabolic clusters provided a better diagnostic tool than the use of individual metabolite measurements. It also demonstrated that the clusters were strongly associated with DMI and the severity of NEB in the first 50 DIM, but only weakly with some milk quality parameters and milk yield in very early lactation.

Another characteristic change over the periparturient period is that immune function is suppressed. Not only do the numbers of circulating leukocytes decrease in early lactation (Cai et al., 1994; Mallard et al., 1998; Wathes et al., 2009) but their functional capacity (e.g., their ability to generate reactive oxygen species *in vitro*) is reduced (Ingvarlsen and Moyes, 2013). This loss of functionality is strongly associated with liver triacylglycerol content and circulating NEFA concentrations, indicators of lipid mobilization (Zerbe et al., 2000; Hammon et al., 2006; McCarthy et al., 2016). A gene expression study of neutrophils obtained from cows with elevated NEFA and BHB levels after calving found that genes important for granulocyte recruitment, IFN signaling, and apoptosis were all downregulated (Crookenden et al., 2019). The impaired immune function is likely to be linked directly to the reduction in nutrient availability. Immune cells require an adequate supply of glucose, amino acids, fatty acids, and cholesterol/oxysterols to mount an effective immune defense (Ingvarlsen and Moyes, 2013; Loftus and Finlay, 2016; Walls et al., 2016). Clonal expansion of T cells in response to antigen recognition also requires dynamic changes in their metabolism (Dimeloe et al., 2017; Desdín-Micó et al., 2018). Immune dysfunction makes cows more susceptible to infectious disease, and a high proportion of dairy cows experience infection of their reproductive tract after calving, which manifests as metritis or endometritis (Sheldon et al., 2006). The incidence of mastitis also increases at this time (Van-groenweghe et al., 2005).

Pathways involving lipid mobilization are all involved in metabolic adaptations necessary for survival during periods of nutrient deprivation or in periparturient animals (Ingvarlsen and Andersen, 2000). In lactating

cows, this involves minimizing glucose utilization and switching to fatty acids (FA) as the main energy source via mobilization of triglycerides stored in adipose tissue (Bauman and Currie, 1980; Contreras et al., 2018). The liver plays a critical role by supplying glucose and ketone bodies to other organs (Shahzad et al., 2014). The metabolic response to fasting is coordinated by the endocrine system with key hormones including insulin, glucagon and GH, and requires induction of enzymes for fatty acid oxidation and ketogenesis. Adenosine monophosphate-activated protein kinase (AMPK) is a serine threonine kinase that is activated by increases in the cellular AMP:ATP ratio caused by metabolic stresses, thus acting as a sensor of cellular energy status (Violet et al., 2006). Once activated itself, AMPK activates ATP-producing catabolic pathways, such as fatty acid oxidation and glycolysis while simultaneously inhibiting energy-consuming biosynthetic pathways, such as protein, FA, and glycogen synthesis.

We hypothesized that cows that experience metabolic imbalance in early lactation are also more susceptible to immune dysfunction at this time, which will be reflected in differences in their leukocyte transcriptome. The study therefore investigated the mechanisms underlying the relationship between metabolic status, liver function and immunity in high yielding multiparous Holstein Friesian dairy cows. Cows were classified into balanced or imbalanced metabolic groups as described previously (De Koster et al., 2019), and RNA sequencing methodology (RNA-Seq) was used to compare the transcriptomes of their livers and circulating leukocytes.

MATERIALS AND METHODS

The data in this study were collected as a part of the Genotype plus Environment (GplusE) FP7-Project (<http://www.gpluse.eu>). All procedures had local ethical approval and complied with the relevant national and EU legislation under the European Union (Protection of Animals used for Scientific Purposes) Regulations 2012 (S.I. No. 543 of 2012). Details of the management of each herd, laboratory analyses, and phenotypic data collection are provided in Krogh et al. (2020). All chemicals were obtained from Sigma Aldrich (Gillingham, UK) unless otherwise stated.

Animals and Sampling

Samples and production data were obtained between calving and 50 d after calving (1–50 DIM) from 130 Holstein Friesian cows (parity 2: $n = 42$; parity 3: $n = 51$; parity ≥ 4 : $n = 37$) in 4 research herds each in different countries in the European Union (Aarhus University, Denmark; University College Dublin Lyons

Research Farm, University College Dublin, Ireland; Agri-Food and Biosciences Institute, Northern Ireland, UK; and Leibniz Institute for Farm Animal Biology, Dummerstorf, Germany). All cows were milked twice daily and their daily yields were recorded. Milk samples were collected twice weekly until 50 DIM and analyzed for composition of protein, fat, and lactose by mid-infrared analysis. The ECM yield was adjusted to 3.5% fat and 3.2% protein using the formula $ECM = (0.327 \times \text{milk kg}) + (12.95 \times \text{fat kg}) + (7.65 \times \text{protein kg})$. Body weights were recorded twice weekly using weigh scales until 50 DIM. Daily individual DMI was recorded using electronic feeding systems. Weekly ration samples collected over the course of the sampling period were dried and shipped for NE_L analysis in a single run (Cumberland Valley Agricultural Services, Waynesboro, PA). The energy input was calculated by multiplying the weekly NE_L density of the ration with the daily DMI of the animal. The energy output was calculated according to the NRC (2001) calculation correcting for NE_M using the last recorded BW of the animal and the most recent fat, protein, and lactose contents, together with the daily milk yield for the NE_L . Energy balance (EBAL) was calculated as described by Krogh et al. (2020).

Analysis of Glucose, NEFA, BHB, and IGF-1

Blood samples were taken around 14 DIM (15 ± 0.1 DIM, mean \pm SEM) and 35 DIM (37 ± 0.1 DIM) into both serum and heparin tubes by jugular or coccygeal venipuncture, separated by centrifugation ($1,600 \times g$ at 4°C for 15 min), and stored at -20°C for subsequent analysis. Laboratory analysis of blood metabolites was performed at the Department of Animal Science, Aarhus University, Denmark. Glucose and NEFA concentrations were determined using enzymatic methods (glucose, ADVIA 1800 Clinical Chemistry System, Siemens Healthcare Diagnostics, Ballerup, Denmark; NEFA, C ACS-ACOD assay method, Fujifilm Wako Diagnostics, Mountain View, CA). Plasma BHB concentrations were determined by measuring absorbance at 340 nm due to the production of NADH at alkaline pH in the presence of BHB dehydrogenase. Intra- and inter-assay CV were, in all cases, <3 and 4%, respectively, for both low and high control samples. Concentrations of IGF-1 were determined in serum by radioimmunoassay at University College Dublin, Ireland, following acid-ethanol extraction using the method previously described by Beltman et al. (2010). Intra-assay CV were 12.4, 7.5, and 9.9% for low, medium, and high control samples, respectively. The corresponding inter-assay CV were 7.8, 3.9, and 9.4%. The sensitivity of the assay, defined as the lowest concentration detectable, was 4 ng/mL.

Liver Biopsy and RNA Preparation

Liver biopsies were collected from all cows in the study at around 14 DIM using a standard operating procedure. First, a 5 × 5 cm area on the right side of the cow at the 10th intercostal, where it crosses a line from mid-humerus to the tuber coxae, was shaved and disinfected, and 10 mL of local anesthetic (Proca-sel, 2%; Selectavet, Dr. Otto Fisher GmbH, Weyarn-Holzolling, Germany) was given. After a minimum of 10 min, a 5-mm incision was made in the skin. Next, a 20-mg liver biopsy was taken through this incision using a Manan Automatic Biopsy system (14 gauge × 17 mm notch; Marmon/MDTech, Gainesville, FL). The biopsy samples were placed in 2-mL screw-capped collection tubes containing 1 mL of RNAlater solution (Qiagen, Hilden, Germany), and initially kept on wet ice before snap-freezing in liquid nitrogen. The incision was closed with a disposable skin stapler (Autosuture, Roual 35W, United States Surgical, Norwalk, CT). Samples were then stored in a freezer at −80°C before shipment to the University of Liège, Belgium (GIGA Research Facility) for extraction. Approximately 20 mg of frozen liver samples was disrupted using a TissueLyzer II homogenizer for 2 min at 30 Hz twice in 600 µL of Buffer RLT with a 5-mm stainless steel bead (Qiagen). Total RNA was extracted from the homogenates using RNeasy Mini kits and QIAcube workstation according to the manufacturer's instructions (Qiagen). Quantity and quality of RNA were evaluated using a QIAxcel capillary electrophoresis device (Qiagen) and NanoDrop 2000 spectrophotometer (Thermo Fisher Scientific, Waltham, MA), respectively. The average RNA concentrations, absorbance ratios at 260 and 280 nm (A260/280), and RNA integrity scores were 337.7 ng/µL, 2.04, and 7.8, respectively, n = 104 (see Supplemental Table 1A for details; <https://rvcrepository.worktribe.com/output/1442087>).

Leukocyte Collection and RNA Preparation

Blood samples were collected into Tempus blood collection tubes (Thermo Fisher, Loughborough, UK) and shaken vigorously for 15 to 20 s immediately upon collection, frozen, and stored at −80°C. They were then shipped to the Royal Veterinary College (Hatfield, UK) for extraction. Tempus tubes were thawed at

room temperature before decanting the contents into 50-mL conical tubes. Whole-blood extraction (containing leukocytes) used Tempus Spin RNA isolation Kits (Thermo Fisher) following the manufacturer's instructions. Quantity and integrity of RNA were assessed using an Agilent BioAnalyzer 2000 (Agilent Technologies UK Ltd., Cheshire, UK) and Agilent RNA 6000 Nano Kit (Agilent). The RNA measurements were validated using a NanoDrop 1000 spectrophotometer (Thermo Fisher). The average RNA concentrations, A260/280 absorbance ratios, and RNA integrity scores were 145.0 ng/µL, 2.09, and 9.2, respectively, n = 105 (see Supplemental Table 1B for details; <https://rvcrepository.worktribe.com/output/1442087>).

Animal Clustering

Metabolic clusters of cows were derived based on the log-transformed and standardized metabolite and hormone concentrations (mean = 0 and SD = 1) of blood glucose, IGF-1, BHB, and NEFA at 14 and 35 DIM. The *k*-means clustering methodology was described in detail by De Koster et al. (2019). Cows with a favorable metabolic profile were grouped as balanced (**BAL**), cows with an unfavorable metabolic profile were grouped as imbalanced (**IMBAL**), and, for this study, the remainder were placed into an intermediate group. Sample size for RNA-Seq was estimated based on achieving 80% power for each test to detect a true difference in expression fold change of at least 1.2, with a group coefficient of variation of 50% and a false discovery rate of 0.05 for testing 20,000 genes. At least 15 cows in each group was required. The distribution of cows between the 3 metabolic groups with RNA-Seq data available from hepatic and blood leukocyte samples is shown in Table 1. Because not all animals used in the original analysis described by De Koster et al. (2019) had associated RNA-Seq data available, data on the metabolite and IGF-1 concentrations, BW, DMI, milk yield, and composition, and calculated energy balance values for each cow used in the present study were reanalyzed by metabolic cluster. Statistical data analysis was carried out using SPSS version 26 (IBM Corp., Armonk, NY). The differences of the above parameters between metabolic clusters for each of 14 and 35 DIM were initially compared using ANOVA with the level of significance set to $P < 0.05$. Where ANOVA

Table 1. Sample sizes for RNA-sequencing (RNA-Seq) analysis according to metabolic clusters

Group	Balanced	Intermediate	Imbalanced	Total
Cows with liver RNA-Seq data	44	44	16	104
Cows with leukocyte RNA-Seq data	42	44	19	105

showed significance, Tukey HSD multiple comparisons were performed to identify the sources of differences. A 2-way ANOVA was also performed to determine the difference between metabolic clusters, DIM (14 or 35 d), and their interactions.

RNA Sequencing

The RNA sequencing libraries were prepared from liver and whole-blood samples using an epMotion liquid handling workstation (Eppendorf, Hamburg, Germany) with the Illumina TruSeq Stranded Total RNA Library Prep Ribo-Zero Gold kit (Illumina Inc., San Diego, CA) at the University of Liege (GIGA Research Facility, Liege, Belgium). Pooled cDNA libraries were sequenced on an Illumina NextSeq 500 sequencer at 75-nt single-end reads to reach an average 30 million reads per sample. Raw data were stored as FASTQ files (Sanger/Illumina 1.9 [Phred +33]) in the EBI ArrayExpress: E-MTAB-9431, E-MTAB-9347, and E-MTAB-9348.

Transcriptomics Pipeline

Reads were trimmed or removed according to base quality using Trimmomatic v. 0.36 (Bolger et al., 2014) and the following setting (SLIDINGWINDOW:4:25 MINLEN:30 LEADING:3 TRAILING:3). The quality of raw and trimmed FASTQ files was assessed with FastQC (<http://www.bioinformatics.babraham.ac.uk/projects/fastqc/>). *Bos taurus* assembly (ARS_UCD1.2), and its corresponding gene set, was used as reference to map reads using the splice aware aligner HISAT2 (Kim et al., 2015). The SAM files were converted to BAM files and coordinate sorted with SAMtools (Li et al., 2009). Picard Tools (<http://picard.sourceforge.net>) were used on the BAM files to remove PCR duplicates, add read group information, sort by chromosome, and create indexes. Reads per protein coding gene were counted with StringTie (Pertea et al., 2015) and expression values were normalized as reads per kilobase million (RPKM).

The RNA-Seq data were analyzed using Partek Genomics Suite software version 7.1 (Partek Inc., St. Louis, MO). The RPKM values were \log_2 transformed. Effect of different herds on gene expression was removed using the function built in Partek Genomics Suite version 7.1. This function calculates the variation attributable to herd and then adjusts the original values to remove the variation. Differences between the 3 metabolic clusters were analyzed by ANOVA following removal of the herd effect. The results presented here are based on the comparison between BAL and IMBAL cows. Differentially expressed genes (DEG) that met the selection criteria ($P < 0.05$ and fold change >1.2) were taken forward

for pathway analysis using DAVID bioinformatics resources version 6.8 (<https://david.ncifcrf.gov/>; Huang et al., 2009a,b). Benjamini-Hochberg (BH) adjustment was used and statistical significance was considered at $P < 0.05$.

RESULTS AND DISCUSSION

In this study, we used a transcriptomics approach to investigate differences in liver and leukocyte function between cows with BAL or IMBAL metabolic profiles in early lactation. This provided insight into how such metabolic adaptations may affect the immune system. The RNA-Seq data were obtained from 105 multiparous cows from 4 herds, each in a different country. This approach increased the heterogeneity in the data, thus reducing the power of the analyses. It also meant, however, that the differences identified should be relevant across a range of genotypes and management practices. A further novel strategy was the use of *k*-means clustering methodology to divide cows into metabolically BAL, IMBAL, or intermediate groups based on circulating concentrations of NEFA, BHB, glucose, and IGF-1 measured in both early and peak lactation. Metabolic imbalance is defined as “a condition where the regulating mechanisms are insufficient for the animals to function optimally leading to a high risk of a complex of digestive, metabolic, and infectious problems” (Ingvarsen, 2006). Although cows from all 3 metabolic groups were included in the RNA-Seq data analysis, the gene transcription results presented here only include the comparison between BAL and IMBAL cows. This was to improve clarity and because understanding the differences between these 2 groups is considered the most biologically relevant.

Metabolic Characteristics of BAL and IMBAL Cows

The BAL cows had significantly higher circulating concentrations of glucose and IGF-1 and significantly lower concentrations of NEFA and BHB than the IMBAL cows at both 14 and 35 DIM (all $P < 0.001$; Table 2). Glucose ($P < 0.001$), and IGF-1 ($P < 0.002$) concentrations increased between these 2 time points, whereas NEFA concentrations decreased ($P < 0.001$). The IMBAL cows were numerically heavier than the BAL cows at 14 DIM but the weight difference was not significant. Dry matter intake was less in IMBAL cows at both time points ($P < 0.01$). Milk yields were similar between these 2 groups, but the milk of the IMBAL cows contained a lower percentage of protein at both time points ($P < 0.001$) and a higher percentage of fat at 35 DIM ($P < 0.01$). The IMBAL cows therefore had the highest ECM yields at 35 DIM (P

Table 2. Characteristics of the 3 clusters of cows: balanced (BAL), imbalanced (IMBAL), and intermediate (INT)^{1,2}

Item	Day 14			Day 35			P-value (Group)	IMBAL	P-value (Group)	P-value (Day)
	BAL	INT	IMBAL	BAL	INT	IMBAL				
Number of cows	43	44	19	43	44	19				
Glucose (mmol/L)	3.60 ± 0.041 ^a	3.37 ± 0.041 ^b	3.27 ± 0.122 ^b	3.88 ± 0.040 ^d	3.56 ± 0.045 ^e	3.37 ± 0.098 ^e	<0.001		<0.001	<0.001
BHB (mmol/L)	0.46 ± 0.026 ^b	0.60 ± 0.027 ^b	1.35 ± 0.262 ^a	0.44 ± 0.023 ^c	0.59 ± 0.036 ^c	1.26 ± 0.156 ^d	<0.001		<0.001	0.50
NEFA (µmol/L)	584 ± 46.7 ^b	764 ± 50.3 ^b	1350 ± 148.5 ^a	372 ± 40.1 ^c	423 ± 44.3 ^c	939 ± 109.9 ^d	<0.001		<0.001	<0.001
IGF-1 (ng/mL)	131.3 ± 6.88 ^a	59.3 ± 5.36 ^b	47.4 ± 5.40 ^b	160.0 ± 8.63 ^d	72.7 ± 4.78 ^e	60.5 ± 6.11 ^e	<0.001		<0.001	0.002
BW (kg)	652 ± 9.8	661 ± 10.3	687 ± 15.7	643 ± 8.3	624 ± 9.1	653 ± 13.8	0.18		0.12	0.005
DMI ³ (kg/d)	20.2 ± 0.51 ^a	17.9 ± 0.41 ^b	17.9 ± 0.65 ^b	23.1 ± 0.53 ^d	19.5 ± 0.57 ^e	18.8 ± 0.86 ^e	0.003		<0.001	<0.001
Milk yield ³ (kg/d)	34.3 ± 0.95	33.8 ± 0.89	36.4 ± 0.72	40.2 ± 1.14	37.6 ± 1.13 ^c	42.2 ± 1.06 ^d	0.38		0.05	<0.001
Milk fat ³ (%)	4.60 ± 0.098	4.62 ± 0.086	4.73 ± 0.168	3.93 ± 0.096 ^f	4.14 ± 0.083	4.42 ± 0.084 ^e	0.73		0.007	<0.001
Milk protein ³ (%)	3.69 ± 0.045 ^a	3.51 ± 0.045 ^b	3.38 ± 0.082 ^c	3.12 ± 0.029 ^d	2.96 ± 0.031 ^e	2.88 ± 0.050 ^f	0.001		<0.001	<0.001
ECM ³ (kg/d)	40.1 ± 1.25	39.0 ± 1.12	41.1 ± 0.88	41.4 ± 1.00	39.4 ± 1.15 ^d	45.6 ± 1.28 ^e	0.58		0.007	0.15
EBAL ³ (MJ/d)	-4.48 ± 0.863 ^a	-8.40 ± 0.650 ^b	-11.70 ± 1.503 ^b	-1.95 ± 0.803 ^d	-5.74 ± 0.745 ^e	-12.41 ± 1.925 ^f	0.005		<0.001	<0.001

^{a-c, d-f}Within row and day, means with different superscripts differ.

¹Values are expressed as means ± SEM. Animals were categorized based on *k*-means clustering of glucose, BHB, nonesterified fatty acids (NEFA), and IGF-1 concentrations measured in blood at around 14 and 35 DIM.

²*P*-values (Group) are based on 1-way ANOVA for each day separately; *P*-values (Day) are based on 2-way ANOVA including group and day. The only significant group × day interaction was for EBAL, where *P* = 0.001.

³Values are 7-d averages. EBAL = energy balance.

< 0.01). The overall EBAL calculations showed that all 3 groups were in NEB at both time points, but the NEB was more severe in the IMBAL group than in the BAL group on both 14 (*P* < 0.01) and 35 DIM (*P* < 0.001). Energy balance was the only measurement to show a significant group × day interaction (*P* < 0.001). For BAL cows, the average improved from -4.48 to -1.95 MJ/d between 14 and 35 DIM, whereas for the IMBAL cows, the values remained poor at both times, at -11.70 and -12.41 MJ/d, respectively. In summary, cows in the IMBAL group were in more severe NEB at both 14 and 35 DIM, which was associated with lower DMI but similar milk yield.

Metabolic adaptation to lactation requires lipolysis of adipose tissue (Bauman and Currie, 1980; Drackley et al., 2001). This is a normal physiological process but in some cows the amount of lipid reaching the liver exceeds its capacity for oxidation or export and triglycerides accumulate, resulting in hepatic steatosis. This impairs liver functionality and increases inflammatory responses (Vernon, 2005). Around half of high-yielding dairy cows are estimated to develop moderate to severe fatty liver disease within the first 14 DIM (Shi et al., 2020). It is therefore probable that a significant proportion of the IMBAL cows in this study were so affected; they also had lower glucose levels. It has been estimated that in cows producing 40 kg of milk/d (similar to the yields in this study), mammary epithelial cells extract up to 2.7 kg/d of glucose from the plasma pool (Bickerstaffe et al., 1974). In ruminants, this glucose demand is met almost exclusively through hepatic gluconeogenesis, placing them at risk of glucose insufficiency during periods of peak demand (Habel and Sundrum, 2020).

A positive correlation was observed between circulating NEFA and BHB concentrations from about 1 wk precalving until 4 wk postpartum, after which concentrations of NEFA generally started to decline, whereas BHB concentrations continue to increase until about wk 6 (Wathes et al., 2007b). Animals that continue to mobilize NEFA for longer in support of lactation lose more condition. The period of high BHB at a time of glucose shortage and with declining blood NEFA reflects utilization of the triacylglycerol, which accumulates in the liver in early lactation to supply energy. A concentration of serum BHB above 1.0 to 1.4 mmol/L is usually considered the threshold for subclinical ketosis, with clinical ketosis occurring at levels >2.0 to 2.6 mmol/L. Symptoms for clinical ketosis include diminished appetite, a decrease in milk yield, and weight loss (Duffield, 2000). Cows with precalving serum NEFA concentrations ≥300 µmol/L are more likely to develop retained placenta and uterine disease, whereas precalving NEFA concentrations >500 µmol/L and postcalving NEFA ≥1,000 µmol/L are associated with an increased risk

of developing a displaced abomasum (Chapinal et al., 2011; Lyons et al., 2014). At least half of all dairy cows are thought to experience subclinical ketosis in the first month of lactation (Duffield, 2000). The IMBAL cows in this study had mean BHB and NEFA concentrations of 1.35 ± 0.262 mmol/L and $1,350 \pm 148.5$ μ mol/L, respectively, at 14 DIM. These values exceeded the accepted thresholds for subclinical ketosis but no cows developed clinical ketosis or a displaced abomasum. Although the EB remained negative in the IMBAL cows at both 14 and 35 DIM, the EB values of around -12 MJ/d at both these time points did not approach the minimum levels of around -40 MJ/d, which cows in severe NEB can reach in early lactation (Taylor et al., 2003; Wathes et al., 2009).

Relationships Between Metabolic Profiles and Gene Expression in Liver

The ANOVA identified 152 DEG, of which 121 genes were upregulated in livers from IMBAL versus BAL cows and 31 were downregulated (Supplemental Tables S2 and S3; <https://rvc-repository.worktribe.com/output/1442087>). The 10 most highly up- or downregulated genes are listed in Tables 3 and 4. Principal component analysis separated the cows into 2 distinct clusters but with some overlap (Supplemental Figure S1). Expression patterns of the 2 groups were, however, distinctly separated using heat map analysis

(Supplemental Figure S2). Analysis of the complete list of DEG using DAVID revealed 5 significant pathways in the functional annotation chart. Two of these pathways also appeared in the only significant functional annotation cluster (BH $P < 0.001$): bta04152: AMPK signaling pathway and bta04922: Glucagon signaling pathway. There was, however, overlap with genes included in bta04920: Adipocytokine signaling pathway and bta04931: Insulin resistance (Tables 5 and 6). The common upregulated DEG in IMBAL cows identified as part of the AMPK, glucagon, and adipocytokine signaling pathways were *CD36*, *CPT1B*, *CREB3L3*, *GYS2*, *LDHB*, *PPARGC1A*, and *RXRG*, which all have well-established roles in regulating metabolic responses to fasting, as described below. Several other DEG, most of which were more highly expressed in the IMBAL cows, were not identified in the functional analysis but are also involved in these processes, as illustrated in Figure 1. These results accord well with previous studies. For example, McCarthy et al. (2010) used differential feeding and milking regimens in early lactation to produce 2 groups of cows with either a mild or severe (SNEB) NEB status. Analysis of array data of hepatic gene expression identified 36 gene networks, of which the 3 most significant were pyruvate metabolism, LXR/RXR activation, and fatty acid metabolism. The most upregulated genes in the SNEB cows included *CPT1B*, *ANGPTL4*, *RXRG*, *APOA1*, and *ACADVL*. Ha et al. (2017) compared the liver transcriptome at 3 time

Table 3. Summary list of the top 10 most upregulated differentially expressed genes in liver and leukocytes in the comparison of cows with imbalanced (IMBAL) versus balanced (BAL) metabolic profiles, sampled at around 14 DIM

Entrez gene	Gene symbol	Gene name	P-value	Fold change
Liver ¹				
509963	<i>ANGPTL4</i>	Angiopoietin like 4	1.70E-05	2.05
537301	<i>APOA4</i>	Apolipoprotein A4	2.80E-03	1.84
509459	<i>CPT1B</i>	Carnitine palmitoyltransferase 1B	1.90E-06	1.78
512633	<i>MFSD2A</i>	Major facilitator superfamily domain containing 2A	3.50E-03	1.77
509500	<i>RXRG</i>	Retinoid X receptor gamma	5.20E-05	1.71
505987	<i>GK</i>	Glycerol kinase	3.70E-03	1.64
505987	<i>INMT</i>	Indolethylamine N-methyltransferase	3.00E-02	1.63
540641	<i>PDK4</i>	Pyruvate dehydrogenase kinase 4	1.80E-04	1.63
540641	<i>NOCT</i>	Nocturnin	1.80E-04	1.6
616337	<i>PLPP5</i>	Phospholipid phosphatase 5	5.50E-03	1.6
Leukocytes ²				
507367	<i>PDK4</i>	Pyruvate dehydrogenase kinase 4	0.000	1.68
404107	<i>DEFB13</i>	Beta-defensin 13	0.017	1.66
280720	<i>BRB</i>	Brain ribonuclease	0.002	1.64
541148	<i>PTX3</i>	Pentraxin 3	0.04	1.58
539835	<i>HSPA6</i>	Heat shock protein family A (Hsp70) member 6	0.003	1.5
101904517	<i>LOC101904517</i>	Multidrug resistance-associated protein 4-like	0.022	1.48
519922	<i>OAS1Z</i>	2',5'-oligoadenylate synthetase 1, 40/46 kDa	0.04	1.45
280692	<i>HP</i>	Haptoglobin	0.03	1.43
282254	<i>HSPA1A</i>	Heat shock 70 kDa protein 1A	0.002	1.42
532668	<i>ZNF821</i>	Zinc finger protein 821	0.002	1.42

¹Liver: BAL, n = 44, IMBAL, n = 16.

²Leukocytes: BAL, n = 42, IMBAL, n = 19.

Table 4. Summary list of the top 10 most downregulated differentially expressed genes in the comparison of cows with imbalanced (IMBAL) versus balanced (BAL) metabolic profiles, sampled at around 14 DIM

Entrez gene	Gene symbol	Gene name	P-value	Fold change
Liver ¹				
513746	<i>SERPINA6</i>	Serpin family A member 6	0.000	-2
281239	<i>IGF1</i>	Insulin like growth factor 1	0.000	-1.62
539466	<i>PPP1R3C</i>	Protein phosphatase 1 regulatory subunit 3C	0.043	-1.52
540473	<i>ASCL1</i>	Achaete-scute family bHLH transcription factor 1	0.013	-1.47
532494	<i>IGFALS</i>	Insulin like growth factor binding protein acid labile subunit	0.022	-1.46
508829	<i>ABCG8</i>	ATP binding cassette subfamily G member	0.02	-1.44
101902412	<i>ANGPTL8</i>	Angiotensinogen like 8	0.011	-1.44
536781	<i>LDB3</i>	LIM domain binding 3	0.047	-1.4
504559	<i>DIRAS3</i>	DIRAS family GTPase 3	0.016	-1.34
280934	<i>SULT1E1</i>	Sulfotransferase family 1E member 1	0.038	-1.33
Leukocytes ²				
504244	<i>TUBA1C</i>	Tubulin, α 1c	0.026	-1.66
100139916	<i>LOC100139916</i>	Interleukin 32-like	0.02	-1.44
280821	<i>JCHAIN</i>	Joining chain of multimeric IgA and IgM	0.027	-1.4
511381	<i>UNG</i>	Uracil DNA glycosylase	0.002	-1.31
514564	<i>ZWINT</i>	ZW10 interacting kinetochore protein	0.016	-1.28
538485	<i>CXXC5</i>	CXXC finger protein 5	0.002	-1.27
509796	<i>DPYSL3</i>	Dihydropyrimidinase like 3	0.022	-1.27
540737	<i>PCLAF</i>	PCNA clamp associated factor	0.028	-1.27
513594	<i>CEP55</i>	Centrosomal protein 55	0.008	-1.26
505233	<i>CERS4</i>	Ceramide synthase 4	0.002	-1.26

¹Liver: BAL, n = 44, IMBAL, n = 16.

²Leukocytes: BAL, n = 42, IMBAL, n = 19.

points with respect to calving: 22 d prepartum and 10 and 17 d postpartum. They also identified *APOA1*, *CPT1B*, *ADIPOR2*, and *CREB3L3* as key genes whose expression changed during the peripartum period, with AMP signaling acting as a central regulator of energy homeostasis.

Lipid Metabolism. Hepatic adaptations in early lactation include upregulation of genes involved in fatty acid oxidation and gluconeogenesis and downregulation of triacylglycerol synthesis (McCarthy et al., 2010; Shahzad et al., 2014). In support of this, the IMBAL cows had greater expression of many genes involved in the uptake, processing, and storage of lipids. Figure 1A shows the pathways involved in triglyceride synthesis and breakdown. Synthesis involves 4 sequential enzymatic steps, of which the third is catalyzed by LPIN1; this gene was more highly expressed in the IMBAL cows. Genes encoding several enzymes potentially involved in the degradation of both triglycerides (*ABHD1*, *BREH1*, *LIPG*) and monoacylglyceride (*MGLL*) into component glycerol and free fatty acids (**FFA**) were upregulated in IMBAL cows. Expression of *GK*, encoding glycerol kinase, also increased.

Alternate pathways that can be used to provide fuel for the tricarboxylic acid (TCA) cycle are summarized in Figure 1B. The *HNF4G* and *ACADVL* genes were both upregulated in IMBAL cows. The HNF4 family are transcription factors that bind FA; HNF4 α regulates the expression of many hepatic genes that influence differentiation and proliferation (Walesky and

Apte, 2015). In mouse intestinal epithelium, HNF4A and HNF4G are both involved in upregulating the acyl-CoA synthetases ACSL5 and ACSF2, which catalyze the conversion of FA into acetyl CoA (Chen et al., 2020). The *ACADVL* gene encodes an acyl-coenzyme A dehydrogenase, which is specific to long-chain and very long chain FA and drives the first step of the mitochondrial fatty acid β -oxidation pathway.

Genes encoding pyruvate dehydrogenase kinase 4 (*PDK4*) and pyruvate carboxylase (*PC*) were also more highly expressed in IMBAL cows; PDK4 inactivates the pyruvate dehydrogenase complex, which catalyzes the conversion of pyruvate to acetyl-CoA (Holness and Sugden, 2003), whereas PC catalyzes the carboxylation of pyruvate to oxaloacetate. Both of these actions help to conserve glucose. Glycogenesis is another glucose-sparing mechanism (Figure 1C). Genes encoding 2 enzymes in this pathway, *UGP2* and *GYS2*, were upregulated. The *PPP1R3C* gene encodes a subunit of the protein phosphatase 1 (PP1) complex, which activates glycogen synthase and limits glycogen breakdown by reducing glycogen phosphorylase activity. This gene was downregulated in the IMBAL cows.

Figure 1D illustrates pathways involving lipid metabolism within the hepatocyte. The gene encoding the adiponectin receptor (*ADIPOR2*) was more highly expressed in IMBAL cows. This mediates increased AMPK and peroxisome proliferator-activated receptor (**PPAR**) ligand activities. The AMP-activated protein kinase is a serine/threonine kinase, and its signaling

Table 5. Functional annotation analysis of genes that showed significant differential expression in liver samples collected from dairy cows with balanced (n = 44) or imbalanced (n = 16) metabolic profiles in early lactation, sampled at around 14 DIM

Category ¹	Term	P-value	BH ²	Fold enrichment	Genes in pathway ³
KEGG_PATHWAY	bia03320:PPAR signaling pathway	1.53E-06	1.73E-04	18.4	ACOX2, ANGPTL4, APOA1, CD36, CPT1B, GK, RXRG
KEGG_PATHWAY	bia04152:AMPK signaling pathway	3.93E-04	0.022	9.2	CD36, CPT1B, CREB3L3, GYS2, IGF1, PPARGC1A
UP_KEYWORDS	Transport	5.05E-04	0.064	2.8	APOA1, APOA4, CD36, CPT1B, CROT, DDX25, KDELR3, MPC1, P2RX4, SERPINA6, SLC1A2, SLC6A11, SLC25A30, SLC25A33, SLC25A34, SLC25A47
KEGG_PATHWAY	bia01100:Metabolic pathways	0.001019	0.038	2.4	ACADVL, ACOX2, AOX1, ALG9, AMDHD1, ARG1, DMGDH, GK, HAL, HDC, IDH1, LDHB, LPINI, MGLL, SHMT2, UGP2
KEGG_PATHWAY	bia04922:Glucagon signaling pathway	0.0015	0.042	9.7	CPT1B, CREB3L3, GYS2, LDHB, PPARGC1A

¹Category terms derived from DAVID bioinformatics resources version 6.8 (<https://david.ncifcrf.gov>).

²P-values with Benjamini-Hochberg adjustment.

³Genes in boldface had higher expression in the imbalanced cows.

Table 6. Functional cluster analysis of the genes that showed significant differential expression in liver samples collected from dairy cows with balanced (n = 44) or imbalanced (n = 16) metabolic profiles in early lactation, sampled at around 14 DIM

Annotation Cluster 1	Term	P-value	BH ²	Genes in pathway ³
KEGG_PATHWAY	bia04152:AMPK signaling pathway	3.93E-04	0.022	CPT1B, CD36, IGF-1, GYS2, CREB3L3, PPARGC1A
KEGG_PATHWAY	bia04922:Glucagon signaling pathway	0.0015	0.042	CPT1B, LDHB, GYS2, CREB3L3, PPARGC1A
KEGG_PATHWAY	bia04931:Insulin resistance	0.0027	0.059	CPT1B, CD36, GYS2, CREB3L3, PPARGC1A
KEGG_PATHWAY	bia04920:Adipocytokine signaling pathway	0.0061	0.095	CPT1B, CD36, RXRG, PPARGC1A

Enrichment score: 2.75

¹Category terms derived from DAVID bioinformatics resources version 6.8 (<https://david.ncifcrf.gov>).

²P-values with Benjamini-Hochberg adjustment.

³Genes in boldface had higher expression in the imbalanced cows.

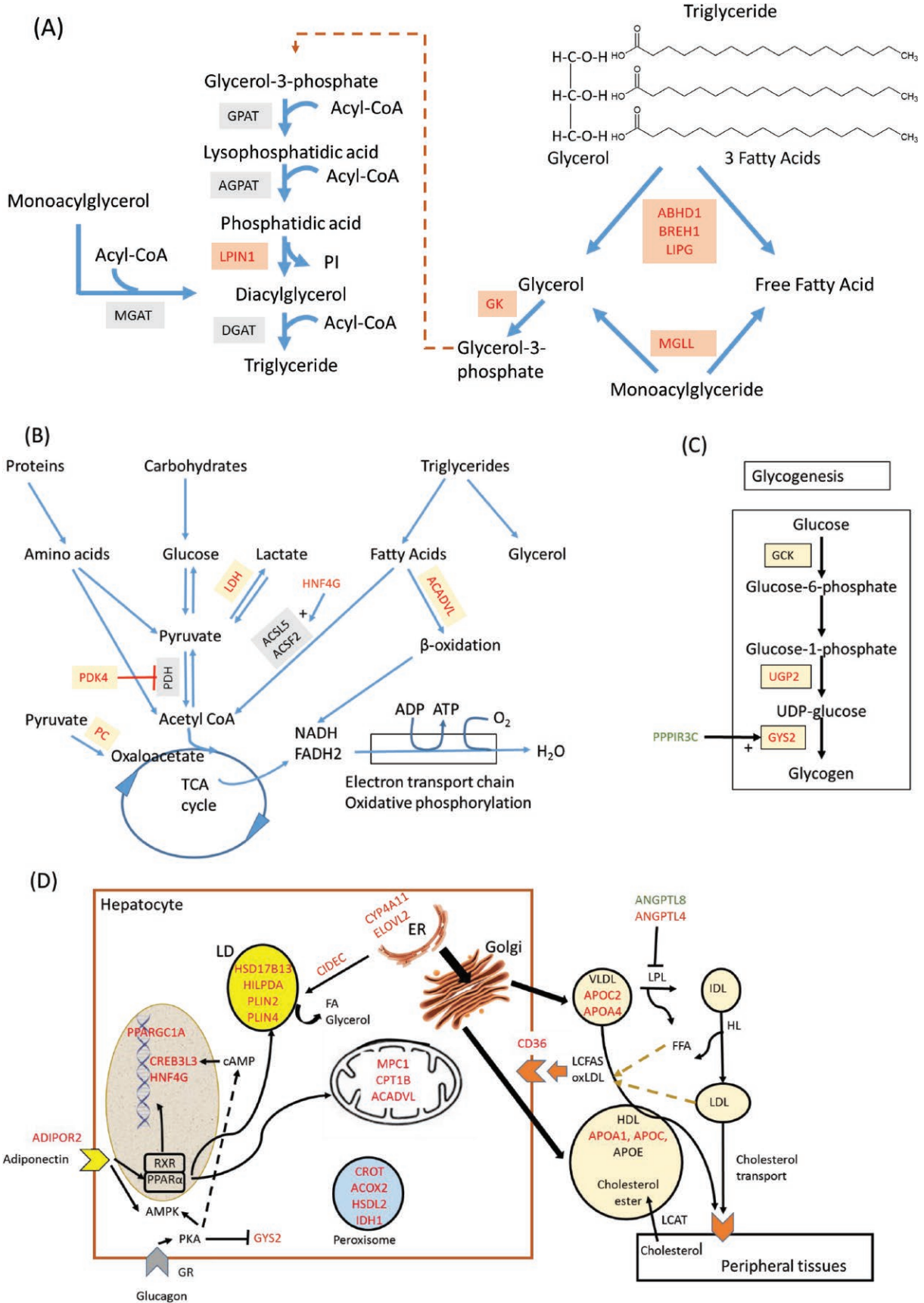


Figure 1. Proteins encoded by genes whose expression was significantly higher in imbalanced (IMBAL; unfavorable metabolic profile) compared with balanced (BAL; favorable metabolic profile) cows are shown in red and those whose expression was lower are in green. (A) Summary of the pathways involved in triglyceride synthesis and breakdown. LPIN1 catalyzes the penultimate step in triglyceride synthesis including the dephosphorylation of phosphatidic acid to yield diacylglycerol. ABHD1, BREH1, LIPG, and MGLL all have lipase activity and are involved in triglyceride or monoacylglyceride metabolism, yielding glycerol and free fatty acids. GK catalyzes the phosphorylation of glycerol by ATP, yielding ADP and glycerol-3-phosphate. (B) Summary of alternative pathways leading from proteins, carbohydrates, or triglycerides to provide fuel for the tricarboxylic acid (TCA) cycle and oxidative phosphorylation. Under anaerobic conditions, pyruvate is converted to lactate with the first step catalyzed by LDH. ACSL5 and ACSF2 catalyze the conversion of long- and medium-chain fatty acids to acetyl-CoA for potential degradation via β -oxidation. These genes are upregulated by the transcription factor HNF4G. The mitochondrial enzyme PDK4 inactivates the pyruvate dehydrogenase complex, which catalyzes the conversion of pyruvate to acetyl-CoA. PC catalyzes the carboxylation of pyruvate to oxaloacetate. Together these changes favor the use of fatty acids and spare glucose for the generation of energy. (C) Pathway of glycogenesis. Two enzymes in this pathway, UGP2 and GYS2, were upregulated in IMBAL cows. These activities also spare glucose use and promote glycogen storage. *PPP1R3C*, which encodes a subunit of the protein phosphatase 1 (PP1) complex, which activates GYS2, was however less highly expressed in IMBAL cows. (D) Pathways involving lipid metabolism within the hepatocyte and lipoproteins. ADIPOR2 mediates increased AMPK and PPAR ligand activities. PPARs can form heterodimers with RXR and bind a PPRE on target genes. CREBL3 has similar and additive actions to PPAR α . The transcription factor HNF4G upregulates ACSL5 and ACSF2 (see Figure 1B). CPT1B transports long-chain fatty acyl-CoAs from the cytoplasm into the mitochondria where ACADVL drives the first step of the fatty acid β -oxidation pathway (Figure 1B). Pyruvate is transported into the mitochondria by a MPC1/MPC2 heterodimer. CYP4A11 localizes to the endoplasmic reticulum (ER) and hydroxylates medium-chain fatty acids. ELOVL2 catalyzes the first and rate-limiting reaction of the long-chain fatty acid elongation cycle. Small cytoplasmic lipid droplets (LD) form by budding off from the ER. CIDEA regulates LD enlargement. PLIN2, PLIN4, HSD17B13, and HILPDA are all involved in regulating the balance between storage and lipolysis within the LD. The 4 enzymes ACOX2, CROT, HSDL2, and IDH1 all play a role in breakdown of fatty acids within peroxisomes, and the transport of medium- and long-chain acyl-CoA molecules back into the cytosol. Hepatocytes also synthesize lipoproteins, which transport lipids, triglycerides, and cholesterol esters around the body. Circulating very low density lipoproteins (VLDL) release FA and glycerol from triglycerides through the actions of lipoprotein lipase (LPL) and hepatic lipase (HL), resulting in formation of intermediate and low density lipoproteins (IDL, LDL) in which the neutral lipid core is progressively depleted of triglyceride and enriched in cholesterol ester. LDL delivers cholesterol to extra-hepatic tissues, whereas high density lipoproteins (HDL) transport cholesterol in the reverse direction back to the liver, where it can be degraded to bile acids and secreted. Genes encoding LPL, apolipoproteins (APO) A1, A4, and C2 were all upregulated in IMBAL cows. The angiotensinogen receptors ANGPTL4 and ANGPTL8 cooperate in regulating LPL activity. CD36 is an adhesion molecule involved in uptake of long-chain fatty acids and oxidized LDL. ABHD1, abhydrolase domain containing 1; AGPAT, 1-acylglycerol-3-phosphate-O-acyltransferase; BREH1, retinyl ester hydrolase type 1; DGAT, diglyceride acyltransferase; GK, glycerol kinase; GPAT, glycerol-3-phosphate acyltransferase; LIPG, lipase; LPIN1, lipin 1; MGLL, monoglyceride lipase. ACADVL, acyl-CoA dehydrogenase, very long chain; ACSL5, acyl-CoA synthetase long chain family member 5; ACSF2, acyl-CoA synthetase family member 2; HNF4G, hepatocyte nuclear factor 4 gamma; LDH, lactate dehydrogenase; PC, pyruvate carboxylase; PDH, pyruvate dehydrogenase; PDK4, pyruvate dehydrogenase kinase 4. GSK3, glycogen synthase kinase 3; GSK3, glycogen synthase kinase 3; GYS2, glycogen synthase; PPP1R3C, protein phosphatase 1 regulatory subunit 3C; UGP2, UDP-glucose pyrophosphorylase 2. ACOX2, acyl-CoA oxidase 2; ADIPOR2, adiponectin receptor 2; ANGPTL4, angiotensinogen receptor like 4; ANGPTL8, angiotensinogen receptor like 8; CIDEA, cell death inducing DFFA like effector c; CPT1B, carnitine palmitoyltransferase 1B; CREBL3, cAMP responsive element binding protein 3 like 3; CROT, carnitine O-octanoyltransferase; cytochrome P450, family 4, subfamily A, polypeptide 11; ELOVL2, fatty acid elongase 2; HILPDA, hypoxia inducible lipid droplet associated; HSD17B13, hydroxysteroid 17 β -dehydrogenase 13; HSDL2, hydroxysteroid dehydrogenase like 2; IDH1, isocitrate dehydrogenase [NADP(+)] 1, cytosolic; MPC1, mitochondrial pyruvate carrier 1; PLIN2, perilipin 2; PLIN4, perilipin 4; PPAR, peroxisome proliferator activated receptor; PPRE, peroxisome proliferator response element; RXR, retinoid X receptor.

pathway acts as a sensor of cellular energy status. It inhibits energy-consuming processes including protein, FA, and glycogen synthesis while activating the ATP-producing catabolic pathways of FA oxidation and glycolysis (Viollet et al., 2006). Peroxisome proliferator-activated receptors are activated by FA and their derivatives and can form heterodimers with retinoid X receptors (RXR) and bind a peroxisome proliferator response element on target genes. Both PPAR α and PPAR γ are expressed in liver and have significant influences on hepatic glucose and lipid metabolism, adipocyte differentiation and inflammatory responses (Grygiel-Górniak, 2014; Nakamura et al., 2014). In the present study, *PPARGC1A* expression was upregulated in IMBAL cows. This gene encodes a transcriptional coactivator that interacts with both PPAR γ and the cAMP response element binding protein (CREB). Shahzad et al. (2014) found that the PPAR signaling pathway was more highly induced postpartum in the livers of cows that had been restricted fed versus overfed during the dry period, indicating a response to

different levels of prepartal dietary energy. The *CREBL3* gene, also upregulated in IMBAL cows, encodes a cAMP-dependent transcription factor that has similar and additive actions to PPAR α in reducing the hepatic expression of genes important for FA oxidation and ketogenesis (Nakagawa et al., 2016); PPAR α contributes to the metabolic adaptation to starvation by inducing genes involved in β -oxidation and ketogenesis (Song et al., 2010). These include *PDK4* (mentioned above) and *CPT1B*, which encodes carnitine palmitoyltransferase 1B, the rate-controlling enzyme that transports long-chain fatty acyl-CoAs from the cytoplasm into the mitochondria. Once there, *ACADVL* drives the first step of the mitochondrial fatty acid β -oxidation pathway. Pyruvate is transported into the mitochondria by a MPC1/MPC2 heterodimer, and *MCPI* was also upregulated. Pathway analysis of the DEGs in liver between BAL and IMBAL cows thus confirmed the key roles of AMPK signaling responses and PPAR ligand activities.

Factors Affecting Lipid Storage. During the early postpartum period, a significant amount of the

NEFA taken up by the liver is esterified into triglycerides and stored in hepatocytes as small cytoplasmic lipid droplets (**LD**). These form by budding off from the endoplasmic reticulum (**ER**) and are coated by several proteins, including perilipins, lipogenic enzymes, lipases, and membrane-trafficking proteins. The gene encoding the cytochrome P450 enzyme *CYP4A11*, which localizes to the ER and hydroxylates medium-chain FA, was upregulated in IMBAL cows. Also localizing to the ER, *ELOVL2* catalyzes the first and rate-limiting reaction of the long-chain FA elongation cycle. Several genes encoding proteins associated with LD were also upregulated in IMBAL cows: *CIDECA*, *HSD17B13*, *HILPDA*, *PLIN2*, and *PLIN4*. Su et al. (2019) previously observed upregulation of *HSD17B13* in human patients and mice with non-alcoholic fatty liver disease. The *CIDECA* protein is thought to increase LD enlargement and restrict lipolysis in cultured human hepatocytes, whereas inhibition of *HILPDA* increases triglyceride and cholesterol accumulation (Breher-Esch et al., 2018). Perilipin 1 coordinates the activation of lipolysis by β -adrenergic stimulation and low circulating insulin levels during fasting, but less is known about the precise roles of perilipin 2 and 4 (Carr and Ahima, 2016). It is likely that there are pools of LD in hepatocytes with distinct lipid and protein composition that may be preferentially used for either storage, energy generation or export, but the specific mechanisms that determine the fate of an individual LD remain to be clarified. Hepatocytes also contain many peroxisomes that absorb intracellular nutrients and contain enzymes involved in FA breakdown. Upregulated genes in IMBAL cows associated with peroxisomes included *ACOX2*, *CROT*, *HSDL2*, and *IDH1*.

Lipoproteins and Cholesterol. The liver also synthesizes lipoproteins, large water-soluble complexes in which the insoluble lipid core is surrounded by a layer of apoproteins, phospholipids and unesterified cholesterol. Surplus triglycerides are initially exported from hepatocytes as very low density lipoproteins (**VLDL**). Once in the circulation, FA and glycerol are released from the triglycerides through the actions of lipases, producing intermediate and low density lipoproteins, in which the neutral lipid core is progressively depleted of triglyceride and enriched in cholesterol ester (Figure 1D). Low density lipoprotein delivers cholesterol to extra-hepatic tissues, whereas high density lipoproteins transport cholesterol in the reverse direction back to the liver, where it can be degraded to bile acids and secreted. Genes encoding the endothelial type lipase *LIPG* and the apolipoproteins (*APO*) *A1*, *A4*, and *C2* were all upregulated in IMBAL cows. Whereas *APOA1* and *APOC2* are major components of high density lipoproteins and VLDL, respectively (Wu et al., 2015),

APOA4 appears to modulate VLDL expansion, enhancing triglyceride loading (Weinberg et al., 2012). Ha et al. (2017) previously reported increased hepatic expression of *APOA1*, *APOA4*, and *APOC2* over the peripartum period in dairy cows, noting that these genes are all associated with cholesterol metabolism and can be linked to FA oxidation and metabolism through the actions of RXRG. These genes are all important in achieving a balance between the uptake and export of FA by the liver during periods of nutrient shortage.

Lipoprotein lipase (LPL) activity is influenced by the secreted angiopoietins whose concentrations in cows are correlated with plasma NEFA (Nakano et al., 2018). In IMBAL cows, expression of *ANGPTL4* increased (and was the most highly upregulated hepatic gene), whereas that of *ANGPTL8* decreased. McCabe et al. (2012) also found that *ANGPTL4* was upregulated in livers of cows in SNEB. Both *ANGPTL4* and *ANGPTL8* inhibit LPL and can form complexes with *ANGPTL3* and with each other. The *ANGPTL4/ANGPTL8* complex is, however, less active than *ANGPTL4* alone (Kovrov et al., 2019; Li et al., 2020); therefore, LPL activity would be predicted to decrease when *ANGPTL8* expression is reduced. The gene encoding ATP binding cassette subfamily G member, *ABCG8*, was upregulated in IMBAL cows. The protein product promotes excretion of cholesterol and sterols from hepatocytes into bile, playing a key role in preventing potentially harmful accumulation of xenosterols (Patel et al., 2018).

Steroid Hormone Activity. The liver also plays a role in steroid hormone homeostasis. This is potentially important in terms of cattle fertility, because circulating estradiol-17 β concentrations must be sufficient to trigger the LH surge and ovulation, whereas the rate of increase in progesterone levels after ovulation is related to the likelihood of conception (Diskin et al., 2006). Corticosteroid binding globulin is the major transport protein for both glucocorticoids and progestins in the blood. It is encoded by *SERPINA6*, which was the most downregulated gene in IMBAL cows, potentially reducing circulating progesterone levels. The *SULT1E1* gene was also in the top 10 list of most downregulated genes in the IMBAL cows (Table 4). This gene encodes an enzyme that inactivates estrogens by sulfation; paradoxically, therefore, its decrease might help to maintain circulating estradiol concentrations. The cholesterol side chain cleavage enzyme *CYP11A1* was upregulated in IMBAL cows. It catalyzes the conversion of cholesterol to pregnenolone, the first step in steroid hormone synthesis. In accord with these results, McCabe et al. (2012) previously noted downregulation of *SULT1E1* and upregulation of *CYP11A1* in livers of postpartum cows experiencing SNEB. Salleh et al. (2017) compared the hepatic transcriptomes of lactat-

ing cows subdivided according to their residual feed intake and found that the steroid hormone biosynthesis pathway, including *CYP11A1*, was upregulated in the group with high residual feed intake. The liver is, however, associated with steroid metabolism rather than biosynthesis, which occurs in specialized glands elsewhere in the body. The *CYP11A1* gene is also involved in vitamin D metabolism (Tuckey et al., 2019). Vitamin D is important for calcium homeostasis in lactation, and circulating concentrations of 25-hydroxyvitamin D are lower in the early postpartum period (Holcombe et al., 2018). Further work is required to determine the potential role of hepatic *CYP11A1* expression in this process.

Endothelial Cells and Inflammation. Another aspect of fatty liver disease is the involvement of cell types in addition to hepatocytes: these include the resident macrophages (Küpfner cells) and sinusoidal endothelial cells. Several of the DEG identified in this study play key roles in the migration of neutrophils from the bloodstream into inflamed tissues, including *PTAFR*, *SELP*, *SEMA4D*, *TNFSF18*, and *VCAM1*, which were all downregulated in IMBAL cows (Supplemental Table S3; <https://rvc-repository.worktribe.com/output/1442087>). Contreras et al. (2012) showed that the addition of NEFA to cultured bovine endothelial cells caused a significant increase in mRNA of cytokines (*IL6*, *IL8*) and adhesion molecules (*ICAM1*, *VCAM1*) associated with inflammatory responses, including leukocyte migration into extravascular tissue. Two previous studies that investigated the transcriptome of white blood cells during the transition period found changes in gene expression related to transendothelial migration. Whereas Minuti et al. (2020) reported activation of this pathway in leukocytes after calving (including increased *VCAM1* expression), Crookenden et al. (2019) found a reduction of migration capacity, indicated by decreased expression of *C5AR1*, *CXCR2*, and *SELL*. This was in accord with our finding of reduced hepatic expression of genes involved in leucocyte migration in IMBAL compared with BAL cows. Such changes could potentially reduce the neutrophil response to inflammatory stimuli in IMBAL cows and imply greater hepatic neutrophil invasion in the BAL cows, although this suggestion requires verification using histological techniques.

Hepatic Somatotrophic System. Insulin-like growth factor-1 is synthesized primarily in the liver, and circulating IGF-1 concentrations in postpartum cows are highly correlated with hepatic *IGF1* expression levels (Fenwick et al., 2008). The *IGF1* and *IGFALS* genes were both in the top 10 list of most downregulated genes in the IMBAL cows (Table 4), whereas *IRS2* (insulin receptor substrate 2) and *IGFBP2* were more highly expressed (Supplemental Table S2). For *INSR*,

$P = 0.052$ but the fold change was -1.09 , implying little difference between the 2 groups. In dairy cows, the somatotrophic axis becomes uncoupled during the peripartum period, so IGF-1 decreases even though GH concentrations increase (Lucy, 2001; Lucy et al., 2009). Insulin concentrations are also lower in early lactation (Wathes et al., 2007b). In addition, adipose tissue and muscle become insulin resistant but develop increased sensitivity to lipolytic agents (De Koster and Opsomer, 2013). In this study, however, expression of the insulin receptor in the liver was unchanged, and *IRS2* was slightly increased in the IMBAL cows. Fenwick et al. (2008) similarly did not find changes in hepatic insulin receptor expression in cows in SNEB, and Zachut et al. (2013) reported that hepatic tissue in early lactating Holstein cows did not exhibit insulin resistance. The *IRS2* gene encodes a cytoplasmic signaling molecule that is phosphorylated by tyrosine kinase upon receptor stimulation and mediates downstream effects of both insulin and IGF-1 (Peng and He, 2018). In contrast, activation of Ser/Thr kinases, leading to serine and threonine phosphorylation of IRS, blocked these pathways and so contributed to pathological insulin resistance. Further work is required to clarify how these complex pathways relating to insulin signaling may be altered in hepatic tissue of cows in early lactation.

In contrast, there is consistent evidence for alterations in the hepatic IGF system in metabolically IMBAL cows. In agreement with the results of the present study, Fenwick et al. (2008) found that early lactation cows in SNEB had reduced hepatic expression of *IGF1*, *IGF1R*, *IGF2R*, 4 of the 6 IGFbps (*IGFBP3*, 4, 5, 6), the acid labile subunit *IGFBPALS*, and the GH receptor (both total *GHR* and the liver specific *GHR1A* variant). Insulin-like growth factor binding protein-3, together with ALS, forms a ternary complex with IGF-1, which is the main carrier protein for IGF-1 in blood, acting to prolong its half-life in the circulation (Clemmons, 1997). In contrast, *IGFBP2* follows the opposite trend, increasing during SNEB, having a negative correlation with circulating IGF-1 and with both hepatic expression and circulating concentrations of *IGFBP2* increasing in early lactation (Vleurick et al., 2000; Fenwick et al., 2008). Insulin-like growth factor binding protein-2 can inhibit the actions of IGFs in cell lines (Höflich et al., 1998) and promotes rapid clearance of IGF from the circulation (Cohick, 1998). It is therefore clear that there is an overall suppression of IGF-1 activity in IMBAL cows in early lactation. This will affect many bodily functions and has been associated with both a reduced likelihood of conception (Taylor et al., 2004) and an increased risk of culling (Lyons et al., 2014). Several other genes that were more highly expressed in IMBAL cows are known targets for

both IGF and insulin signaling with respect to glucose metabolism and have already been mentioned. These included *CPT1B*, *CREB3L3*, *GYS2*, *RXRG*, *PPARG-C1A*, *CD36*, *ADIPOR2*, and *LDHA*.

Relationships Between Metabolic Profiles and Gene Expression in Leukocytes

There were 59 upregulated and 58 downregulated DEG identified in the leukocytes of IMBAL versus BAL cows (Supplemental Tables S4 and S5; <https://rvc-repository.worktribe.com/output/1442087>). The top 10 genes in each category are listed in Tables 3 and 4. Principal component analysis separated the cows into 2 distinct clusters (Supplemental Figure S3). The somewhat greater overlap of distribution for the leukocyte samples compared with the liver samples was expected, because the groups were defined on the basis of circulating metabolites, and many other factors will also influence expression patterns, particularly in leukocytes. A heat map analysis is given in Supplemental Figure S4 and confirms clear differences in overall gene expression patterns of leukocytes between the 2 groups. The DAVID analysis of the list of DEG revealed 7 significant UP_keyword terms: chromosome, nucleosome core, DNA-binding, methylation, citrullination, nucleus, and stress response (fold enrichment 16.1 to 2.2, BH 3.55E-08 to 4.5E-03; Table 7). The top annotation cluster similarly included the terms chro-

mosome, histone core, and nucleosome core (Table 8). This cluster included 26 genes that were more highly expressed in BAL cows, of which 11 encoded histones (Table 9). These are the main proteins in chromatin that package DNA into nucleosomes; their posttranslational modification by acetylation, methylation, and phosphorylation plays a central role in controlling gene transcription. In terms of immune responses, histone methylation is important for orchestrating the pathways that regulate differential development of effector and memory T cells and cytokine production (He et al., 2013). Other DEG in cluster 1 more highly expressed in BAL cows were involved in aspects of cell division (*BIRC5*, *CCNB1*, *CCNE2*, *CDC20*, *SKA2*, *UBE2C*, *ZWINT*) and DNA repair (*POLE2*, *UNG*). Of these, *BIRC5* encodes a protein termed “survivin” that acts as an inhibitor of apoptosis and is essential for successful cell division (Altieri, 2015). The 12 genes more highly expressed in the IMBAL cows had more varied actions, including regulating cell cycle progression (*CDKN1A*, *PFKFB30*), heat shock proteins (**HSP**; *DNAJB1*, *HSPB1*), and transcription factors (*CEBPB*, *FOXS1*, *IRF7*, *ZNF821*). Cluster 3 included the terms cell division, cell cycle, and mitosis. All 9 genes in this cluster were also present in cluster 1 (Table 9).

Cluster 2 included the terms heat shock protein and stress response (Table 8), with 9 of the 10 genes upregulated in IMBAL cows (Table 9). These included 5 HSP (*DNAJB1*, *HSPA1A*, *HSPA6*, *HSPB1*, *HSPH1*) but

Table 7. Functional annotation analysis of the genes that showed significant differential expression in leukocyte samples collected from dairy cows with balanced (n = 42) or imbalanced (n = 19) metabolic profiles in early lactation, sampled at around 14 DIM

Category ¹	Term	Count	Fold enrichment	P-value	BH ²
UP_KEYWORDS	Chromosome	14	11.25	3.0E-10	3.5E-08
INTERPRO	IPR007125:Histone core	9	18.40	2.8E-08	6.5E-06
KEGG_PATHWAY	bta05322:Systemic lupus erythematosus	12	8.78	6.6E-08	7.8E-06
UP_KEYWORDS	Nucleosome core	9	16.09	8.2E-08	4.9E-06
INTERPRO	IPR009072:Histone-fold	9	13.17	3.8E-07	4.5E-05
KEGG_PATHWAY	bta05034:Alcoholism	12	7.27	4.5E-07	2.7E-05
KEGG_PATHWAY	bta05203:Viral carcinogenesis	12	6.68	1.1E-06	4.1E-05
UP_SEQ_FEATURE	chain:Histone H2B type 1	6	28.57	1.5E-06	1.9E-04
UP_SEQ_FEATURE	chain:Histone H2B type 1-N	6	28.57	1.5E-06	1.9E-04
INTERPRO	IPR000558:Histone H2B	6	26.11	3.0E-06	2.3E-04
SMART	SM00427:H2B	6	21.69	6.7E-06	4.7E-04
GOTERM_CC_DIRECT	GO:0000788~nuclear nucleosome	6	21.08	8.7E-06	1.0E-03
GOTERM_BP_DIRECT	GO:0006334~nucleosome assembly	8	10.18	1.2E-05	6.5E-03
UP_KEYWORDS	DNA-binding	17	3.54	1.9E-05	7.6E-04
UP_SEQ_FEATURE	cross-link:Glycyl lysine isopeptide (Lys-Gly) (interchain with G-Cter in ubiquitin)	8	8.08	4.2E-05	2.8E-03
INTERPRO	IPR018181:Heat shock protein 70, conserved site	4	48.49	6.7E-05	3.9E-03
INTERPRO	IPR013126:Heat shock protein 70 family	4	48.49	6.7E-05	3.9E-03
GOTERM_CC_DIRECT	GO:0000786~nucleosome	6	12.05	1.3E-04	8.0E-03
UP_KEYWORDS	Methylation	10	5.06	1.5E-04	4.5E-03
UP_KEYWORDS	Citrullination	5	18.26	1.5E-04	3.7E-03
UP_KEYWORDS	Nucleus	26	2.16	2.3E-04	4.5E-03
UP_KEYWORDS	Stress response	5	15.85	2.7E-04	4.5E-03

¹Category terms derived from DAVID bioinformatics resources version 6.8 (<https://david.ncifcrf.gov>).

²P-values with Benjamini-Hochberg adjustment.

also *TLR4*, a bacterial pathogen recognition receptor; the cytokine *IL12B*, the suppressor of cytokine signaling *SOCS1*; and *IRF7*, an IFN regulatory transcription factor that is important in response to viral infection. In humans, these genes participate in several Kyoto Encyclopedia of Genes and Genomes (KEGG) pathways involved in responses to a variety of pathogens (bta05162:Measles; bta05134:Legionellosis; bta05145:Toxoplasmosis; bta05164:Influenza A; bta04620:Toll-like receptor signaling pathway; Table 8). During the early postpartum period, the metabolic imbalances experienced, together with possible pathogen exposure, are likely to place increased demands on the immune system, which includes a requirement for protein synthesis. If these proteins are misfolded or aberrantly modified then they cannot exit the ER lumen and so cause ER stress. During such an unfolded protein re-

sponse, overall mRNA translation is inhibited but more molecular chaperones are produced to help correct folding of the proteins that are being made (Clerico et al., 2015). The 5 HSP upregulated in the IMBAL cow leukocytes are all involved in providing protection from misfolded proteins. In addition to this role, HSP are also involved in immune responses, in part by binding pathogen-associated molecular pattern (PAMP) molecules and modulating PAMP-induced toll-like receptor signaling (Osterloh and Breloer, 2007).

Other notable DEG not part of these 3 clusters (listed in Supplemental Tables S4 and S5) included those with involvement in glucose metabolism: expression of the adipokine *C1QTNF12* was higher in the BAL cows whereas *PDK4* and *PFKFB3* were both lower. Expression of *IGF2BP3* was downregulated in the IMBAL cows. Other DEG were involved in immune

Table 8. Functional cluster analysis of the genes that showed significant differential expression in leukocyte samples collected from dairy cows with balanced (n = 42) or imbalanced (n = 19) metabolic profiles in early lactation, sampled at around 14 DIM

Cluster and category	Term	Count	P-value	BH ²
Annotation Cluster 1	Enrichment score: 4.67			
Category ¹				
UP_KEYWORDS	Chromosome	14	3.0E-10	3.5E-08
INTERPRO	IPR007125:Histone core	9	2.8E-08	6.5E-06
KEGG_PATHWAY	bta05322:Systemic lupus erythematosus	12	6.6E-08	7.8E-06
UP_KEYWORDS	Nucleosome core	9	8.2E-08	4.9E-06
INTERPRO	IPR009072:Histone-fold	9	3.8E-07	4.5E-05
KEGG_PATHWAY	bta05034:Alcoholism	12	4.5E-07	2.7E-05
KEGG_PATHWAY	bta05203:Viral carcinogenesis	12	1.1E-06	4.1E-05
UP_SEQ_FEATURE	chain:Histone H2B type 1-N	6	1.5E-06	1.9E-04
UP_SEQ_FEATURE	chain:Histone H2B type 1	6	1.5E-06	1.9E-04
INTERPRO	IPR000558:Histone H2B	6	3.0E-06	2.3E-04
SMART	SM00427:H2B	6	6.7E-06	4.7E-04
GOTERM_CC_DIRECT	GO:0000788~nuclear nucleosome	6	8.7E-06	1.0E-03
GOTERM_BP_DIRECT	GO:0006334~nucleosome assembly	8	1.2E-05	6.5E-03
UP_KEYWORDS	DNA-binding	17	1.9E-05	7.6E-04
UP_SEQ_FEATURE	cross-link:Glycyl lysine isopeptide (Lys-Gly) (interchain with G-Cter in ubiquitin)	8	4.2E-05	2.8E-03
GOTERM_CC_DIRECT	GO:0000786~nucleosome	6	1.3E-04	8.0E-03
UP_KEYWORDS	Methylation	10	1.5E-04	4.5E-03
UP_KEYWORDS	Nucleus	26	2.3E-04	4.5E-03
UP_KEYWORDS	Ubl conjugation	11	1.2E-03	1.8E-02
UP_KEYWORDS	Acetylation	19	4.4E-03	4.3E-02
Annotation Cluster 2	Enrichment Score: 2.03			
Category				
INTERPRO	IPR013126:Heat shock protein 70 family	4	6.7E-05	0.004
INTERPRO	IPR018181:Heat shock protein 70, conserved site	4	6.7E-05	0.004
UP_KEYWORDS	Stress response	5	2.7E-04	0.005
KEGG_PATHWAY	bta05162:Measles	7	6.1E-04	0.018
KEGG_PATHWAY	bta05134:Legionellosis	5	8.6E-04	0.020
KEGG_PATHWAY	bta05145:Toxoplasmosis	6	1.5E-03	0.030
KEGG_PATHWAY	bta05164:Influenza A	7	1.8E-03	0.030
Annotation Cluster 3	Enrichment Score: 1.98			
Category				
UP_KEYWORDS	Cell division	6	0.002	0.025
UP_KEYWORDS	Cell cycle	7	0.002	0.029
UP_KEYWORDS	Mitosis	5	0.003	0.034

¹Category terms derived from DAVID bioinformatics resources version 6.8 (<https://david.ncicrf.gov>).

²P-values with Benjamini-Hochberg (BH) adjustment. Only terms significant with BH adjustment are included.

Table 9. List of differentially expressed genes in functional clusters in leukocyte samples collected from dairy cows with balanced (n = 42) or imbalanced (n = 19) metabolic profiles in early lactation,¹ sampled at around 14 DIM (see Table 7 for further details)

Cluster	Genes
Cluster 1: Enrichment Score: 4.67 Top terms: chromosome, histone core	<i>BIRC5</i> , <i>CCNB1</i> , <i>CCNE2</i> , <i>CDC20</i> , <i>CERS4</i> , <i>CXXC5</i> , <i>H2B</i> , <i>HIST1H1A</i> , <i>HIST1H1D</i> , <i>HIST1H2AG</i> , <i>HIST1H2AH</i> , <i>HIST1H2BB</i> , <i>HIST1H2BI</i> , <i>HIST1H2BJ</i> , <i>HIST1H2B3</i> , <i>JCHAIN</i> , <i>LMO2</i> , <i>LOC104968446</i> , <i>LOC516742</i> , <i>MND1</i> , <i>POLE2</i> , <i>SKA2</i> , <i>TUBA1C</i> , <i>UBE2C</i> , <i>UNG</i> , <i>ZWINT</i> , <i>CD36</i> , <i>CDKN1A</i> , <i>CEBPB</i> , <i>DNAJB1</i> , <i>FOXSI</i> , <i>GATM</i> , <i>HSPB1</i> , <i>IRF7</i> , <i>MTUS1</i> , <i>PFKFB3</i> , <i>RGS9</i> , <i>ZNF821</i>
Cluster 2: Enrichment Score: 2.03 Top terms: Heat shock protein 70 family, stress response	<i>CCNE2</i> , <i>DNAJB1</i> , <i>HSPA1A</i> , <i>HSPA6</i> , <i>HSPB1</i> , <i>HSPH1</i> , <i>IL12B</i> , <i>IRF7</i> , <i>SOCS1</i> , <i>TLR4</i>
Cluster 3: Enrichment Score: 1.98 Top terms: cell division, cell cycle	<i>BIRC5</i> , <i>CCNB1</i> , <i>CCNE2</i> , <i>SKA2</i> , <i>TUBA1C</i> , <i>UBE2C</i> , <i>ZWINT</i> , <i>HSPB1</i> , <i>MTUS1</i>

¹Genes in boldface had higher expression in the imbalanced cows.

defense mechanisms. Those more highly expressed in BAL cows included *ACOD1*, *CR2*, *ITGAD*, *JCHAIN*, *LOC100139916* (interleukin 32-like), *LOC100295645*, and *TLR10*. Those that were higher in the IMBAL cows included *CLEC1B*, *DEFB13*, *FCGRT*, *HP*, *IL1RAP*, *KLRA1*, *LOC514978* (LPS binding protein), *LOC618409*, *LOC100852090*, *LOC112445498*, *LOC618409* (interferon regulatory factor 4), *OAS1Z*, *PTX3*, *RAB20*, *RNASE6*, *SEMAD4D*, and *SLC11A1*. Of these, *DEFB13*, *PTX3*, *OAS1Z*, and *HP* were all in the top 10 list (Table 3). The encoded proteins β -defensin 13, pentraxin 3, and haptoglobin all have antimicrobial activity (Mantovani et al., 2008; Mayasari et al., 2017), and *OAS1Z* encodes an IFN response gene that is an effector in the OAS1-RNaseL antiviral pathway (Sadler and Williams, 2008). The IMBAL cows therefore showed more evidence of responses to both bacterial and viral infections and the ER stress response to unfolded proteins.

Several previous studies have investigated changes in gene expression in white blood cells in dairy cows over the peripartum period. Agrawal et al. (2017) compared the transcriptome of bovine polymorphonuclear leukocytes at -14 and +7 DIM between control cows and those overfed a moderate-energy diet during the dry period. They found downregulated expression of *TLR4* and *KLF11* in the overfed cows, whereas *HSPA1A* was upregulated. In our study, all 3 of these genes were more highly expressed in the IMBAL cows. Crookenden et al. (2016) looked at time-dependent changes in gene expression of circulating neutrophils between -1 wk (prepartum) and +4 wk (postpartum) and reported that *TLR4* decreased around calving. Other studies have investigated the leukocyte transcriptome in relation to blood biomarkers around calving. Expression of *TLR4* in mononuclear cells increased after calving, whereas, in agreement with our data, *TLR10* expression declined (Mann et al., 2019). Minuti et al. (2020) found that metabolic pathways related to lipid and amino acid metabolism were inhibited over the immediate postcalving period and immune pathways were activated. Interestingly, as plasma BHB increased, the KEGG pathways relating to DNA replication, cell cycle, homologous recombination, base excision repair, and valine, leucine, and isoleucine biosynthesis were all inhibited, whereas genes involved with vitamin metabolism, the endocrine system, signaling molecules, and the immune system were activated. This is supported by Crookenden et al. (2019), who compared cows classified as being at a high or low risk of metabolic dysfunction. Gene expression patterns in neutrophils isolated from the high-risk cows indicated that apoptosis and cell death were decreased but cell survival time was increased, suggesting that neutrophils survive longer in the circulation when they

are exposed to proinflammatory conditions. Together, these studies suggest that leukocytes in cows with BAL metabolic profiles are more actively engaged in cell division, repair, and protein biosynthesis.

It is notable that several of these studies reported differences in *TLR4* expression between groups or times. In addition to acting as a cell surface receptor that generates innate immune responses to pathogens, TLR4 plays an important role in chronic inflammation by dampening insulin actions both directly, through activation of proinflammatory kinases and reactive oxygen species, and indirectly, via activation of cytokine signaling cascades (Kim and Sears, 2010). It is likely that its inhibitory role in insulin signaling can be activated by saturated fatty acids without the requirement for a pathogen. Potential ligands include palmitic acid (Mamedova et al., 2013), which is a major component of circulating NEFA in the cow. This could in part explain the higher *TLR4* expression in the leukocytes of IMBAL cows, and would contribute to reduced insulin signaling in these cells.

DEG Common to Both Leukocytes and Liver

Four genes were significantly upregulated in the IMBAL cows in both the hepatic and leukocyte data sets: *CD36*, *KLF11*, *PDK4*, and *RAB20*. The key role for PDK4 in helping to conserve glucose by limiting the conversion of pyruvate to acetyl-CoA was mentioned above. CD36 is a multifunctional adhesion molecule present on the cell surface. In the context of energy metabolism its role as a class B scavenger receptor that facilitates the intracellular uptake of long chain FA and oxidized low density lipoproteins seems likely to be most important (Nakamura et al., 2014). The *KLF11* gene encodes Kruppel-like factor 11, a zinc finger transcription factor that binds to and regulates promoters of many genes involved in the metabolism of cholesterol, lipid, and glucose metabolism, including phosphoenolpyruvate carboxykinase (PEPCK) and peroxisome proliferator-activated receptor γ coactivator-1 α (PGC-1 α), subsequently decreasing the cellular output of glucose (Zhang et al., 2014). There is little information available concerning the function of the RAS-related protein *RAB20*, but in human and mouse skeletal muscle, loss of *RAB20* was shown to impair insulin-stimulated glucose uptake by blocking the translocation of GLUT4 to the cell surface (Görgens et al., 2017). Expression of *CPT1A* was higher in leukocytes and that of *CPT1B* was higher in liver. As noted above, carnitine palmitoyltransferases are rate-controlling enzymes in the mitochondrial oxidation of long-chain FA. No genes were significantly downregulated in both leukocytes and liver from IMBAL cows, although there was one

pair of closely related genes: expression of *DIRAS2* was lower in blood and *DIRAS3* was in the top 10 list of most downregulated genes in liver. The DIRAS family members encode GTPases, which compete with RAS for binding to deactivate multiple downstream effect targets of the RAS signaling pathway and they can also interfere with other key signaling pathways including JAK/STAT, PI-3K/AKT, mTOR, and NF- κ B signal transduction (Li et al., 2019). This suggests that RAS signaling may be important in regulating responses to an energy deficit, an aspect that is worth further investigation.

Causes and Consequences of Metabolic Imbalance

The weak relationship between milk yield and metabolic imbalance found in this study supports the earlier findings of Ingvarlsen (2006), who concluded that the important difference between animals is in their ability to cope with the metabolic challenges of early lactation rather than actual milk yield. Some of the differing metabolic responses between cows after calving have been influenced by genetic selection, which has led to alterations in carbohydrate and lipid metabolism and the somatotrophic axis to support higher milk yield potential (e.g., Grisart et al., 2002; Chagas et al., 2007; Wathes et al., 2012). The influence of dry cow management is also of critical importance, as demonstrated by Shahzad et al. (2014), who performed a comprehensive analysis of hepatic transcriptome data obtained over the peripartur period from several experiments that evaluated the effect of prepartur plane of energy intake. Livers from animals that had been on a restricted diet had a greater lipid and amino acid catabolic capacity after calving and a better capacity to cope with ER stress, whereas the overfed animals had a greater activation of pathways and functions related to triglyceride synthesis. Dry matter intake is also of importance and is linked to metabolism, as hepatic oxidation of certain FFA may trigger a satiety signal and so depress feed intake (Ingvarlsen and Andersen, 2000; Hayirli et al., 2002). Restricted feed intake after calving promotes the development of clinical ketosis and is associated with downregulation of genes involved in oxidative phosphorylation, protein ubiquitination, proton transport, cholesterol metabolism, growth hormone signaling, and FA desaturation. Genes involved in cytokine signaling and FA uptake, transport, and oxidation are, however, upregulated (Loor et al., 2006; McCabe et al., 2012).

Our results confirm that appropriate liver function is critical to the success with which a cow transitions into lactation. The BAL cows were able to maintain IGF-1 secretion in early lactation, which in turn is known to be beneficial for fertility. In contrast, the IMBAL cows

clearly had greater problems in maintaining glucose homeostasis and were mobilizing more lipid from body reserves. This promotes the build-up of fat in the liver, which then perturbs other key liver functions, including cholesterol metabolism and glycogen storage. Previous studies have described mechanisms whereby metabolic imbalance can predispose cows to an increased incidence of other diseases, including milk fever, ketosis, and mastitis (Ingvarsen et al., 2003). Habel and Sundrum (2020) presented evidence for the key role of glucose availability in this relationship, as selection of cows for milk yield has prioritized glucose supply to the mammary gland, so reducing its availability to the immune cell population. Our results support these conclusions by providing evidence of impaired functionality of leukocytes in cows with IMBAL metabolic profiles, which was associated with gene expression indicative of reduced glucose availability, reduced cell division, and an increased unfolded protein response. The relationships between nutrient supply, inflammation, and disease are complex, with evidence that some FA are able to activate TLR4 signaling pathways (Kim and Sears, 2010; Mamedova et al., 2013). Furthermore, infections such as *Escherichia coli*-induced mastitis have major systemic effects that impair metabolic hepatic function through altered expression of key regulatory transcription factors including PPAR, RXR, and HNF4A (Heimes et al., 2020). All of these genes were differentially expressed between BAL and IMBAL cows in our study. It is worth noting that, although the IMBAL cows in this study were in a greater energy deficit than the BAL cows, their EB values of around -12 MJ/d were much better than the minimum values of around -40 MJ/d that can be reached in early lactation (Taylor et al., 2003). This suggests that the adverse effects noted here could be much more severe in some animals.

CONCLUSIONS

This study compared the transcriptomes of early postpartum cows showing balanced (high glucose, high IGF-I, low NEFA, and low BHB) and imbalanced (low glucose, low IGF-I, high NEFA, and high BHB) metabolic profiles. Metabolic imbalances in individual cows reflect both their specific genetic and environmental circumstances and the interactions between them. Excessive lipid mobilization and an overall shortage of glucose in some animals compromise their health and productivity. Avoidance of these issues in future dairy production requires a combined approach on the part of breeding companies and farm managers, to select more robust cows and to improve lifetime nutritional management (as heifers and during both lactation and the

dry period). This should be optimized on an individual cow basis, an ideal that should become more feasible in future as better automated monitoring systems are developed.

ACKNOWLEDGMENTS

This project received funding from the European Union's Seventh Framework Programme (Brussels, Belgium) for research, technological development, and demonstration under grant agreement no. 613689. The views expressed in this publication are the sole responsibility of the authors and do not necessarily reflect the views of the European Commission. The authors have not stated any conflicts of interest.

REFERENCES










- Agrawal, A., M. J. Khan, D. E. Graunard, M. Vailati-Riboni, S. L. Rodriguez-Zas, J. S. Osorio, and J. J. Loo. 2017. Prepartal energy intake alters blood polymorphonuclear leukocyte transcriptome during the periparturient period in Holstein cows. *Bioinform. Biol. Insights* 11:1177932217704667. <https://doi.org/10.1177/1177932217704667>.
- Altieri, D. C. 2015. Survivin—The inconvenient IAP. *Semin. Cell Dev. Biol.* 39:91–96. <https://doi.org/10.1016/j.semcdb.2014.12.007>.
- Bach, L. A. 2018. 40 Years of IGF1: IGF-binding proteins. *J. Mol. Endocrinol.* 61:T11–T28. <https://doi.org/10.1530/JME-17-0254>.
- Bauman, D. E. 1999. Bovine somatotropin and lactation: From basic science to commercial application. *Domest. Anim. Endocrinol.* 17:101–116. [https://doi.org/10.1016/S0739-7240\(99\)00028-4](https://doi.org/10.1016/S0739-7240(99)00028-4).
- Bauman, D. E., and W. B. Currie. 1980. Partitioning of nutrients during pregnancy and lactation—A review of mechanisms involving homeostasis and homeorhesis. *J. Dairy Sci.* 63:1514–1529. [https://doi.org/10.3168/jds.S0022-0302\(80\)83111-0](https://doi.org/10.3168/jds.S0022-0302(80)83111-0).
- Bell, A. W. 1995. Regulation of organic nutrient metabolism during transition from late pregnancy to early lactation. *J. Anim. Sci.* 73:2804–2819. <https://doi.org/10.2527/1995.7392804x>.
- Beltman, M. E., N. Forde, P. Furney, F. Carter, J. F. Roche, P. Lonergan, and M. A. Crowe. 2010. Characterisation of endometrial gene expression and metabolic parameters in beef heifers yielding viable or non-viable embryos on Day 7 after insemination. *Reprod. Fertil. Dev.* 22:987–999. <https://doi.org/10.1071/RD09302>.
- Bickerstaffe, R., E. F. Annonson, and J. L. Linzell. 1974. The metabolism of glucose, acetate, lipids and amino acids in lactating dairy cows. *J. Agric. Sci.* 82:71–85. <https://doi.org/10.1017/S0021859600050243>.
- Bolger, A. M., M. Lohse, and B. Usadel. 2014. Trimmomatic: A flexible trimmer for Illumina sequence data. *Bioinformatics* 30:2114–2120. <https://doi.org/10.1093/bioinformatics/btu170>.
- Breher-Esch, S., N. Sahini, A. Trincone, C. Wallstab, and J. Borlak. 2018. Genomics of lipid-laden human hepatocyte cultures enables drug target screening for the treatment of non-alcoholic fatty liver disease. *BMC Med. Genomics* 11:111. <https://doi.org/10.1186/s12920-018-0438-7>.
- Cai, T. Q., P. G. Weston, L. A. Lund, B. Brodie, D. J. McKenna, and W. C. Wagner. 1994. Association between neutrophil functions and periparturient disorders in cows. *Am. J. Vet. Res.* 55:934–943.
- Carr, R. M., and R. S. Ahima. 2016. Pathophysiology of lipid droplet proteins in liver diseases. *Exp. Cell Res.* 340:187–192. <https://doi.org/10.1016/j.yexcr.2015.10.021>.
- Chagas, L. M., J. J. Bass, D. Blache, C. R. Burke, J. K. Kay, D. R. Lindsay, M. C. Lucy, G. B. Martin, S. Meier, F. M. Rhodes, J. R. Roche, W. W. Thatcher, and R. Webb. 2007. Invited review:

- New perspectives on the roles of nutrition and metabolic priorities in the subfertility of high-producing dairy cows. *J. Dairy Sci.* 90:4022–4032. <https://doi.org/10.3168/jds.2006-852>.
- Chapinal, N., M. Carson, T. F. Duffield, M. Capel, S. Godden, M. Overton, J. E. P. Santos, and S. J. LeBlanc. 2011. The association of serum metabolites with clinical disease during the transition period. *J. Dairy Sci.* 94:4897–4903. <https://doi.org/10.3168/jds.2010-4075>.
- Chen, L., R. P. Vasoya, N. H. Toke, A. Parthasarathy, S. Luo, E. Chiles, J. Flores, N. Gao, E. M. Bonder, X. Su, and M. P. Verzi. 2020. HNF4 regulates fatty acid oxidation and is required for renewal of intestinal stem cells in mice. *Gastroenterology* 158:985–999.e9. <https://doi.org/10.1053/j.gastro.2019.11.031>.
- Clemmons, D. R. 1997. Insulin-like growth factor binding proteins and their role in controlling IGF actions. *Cytokine Growth Factor Rev.* 8:45–62. [https://doi.org/10.1016/S1359-6101\(96\)00053-6](https://doi.org/10.1016/S1359-6101(96)00053-6).
- Clerico, E. M., J. M. Tilitky, W. Meng, and L. M. Gierasch. 2015. How hsp70 molecular machines interact with their substrates to mediate diverse physiological functions. *J. Mol. Biol.* 427:1575–1588. <https://doi.org/10.1016/j.jmb.2015.02.004>.
- Cohick, W. S. 1998. Role of the insulin-like growth factors and their binding proteins in lactation. *J. Dairy Sci.* 81:1769–1777. [https://doi.org/10.3168/jds.S0022-0302\(98\)75746-7](https://doi.org/10.3168/jds.S0022-0302(98)75746-7).
- Contreras, G. A., W. Raphael, S. A. Mattmiller, J. Gandy, and L. M. Sordillo. 2012. Nonesterified fatty acids modify inflammatory response and eicosanoid biosynthesis in bovine endothelial cells. *J. Dairy Sci.* 95:5011–5023. <https://doi.org/10.3168/jds.2012-5382>.
- Contreras, G. A., C. Strieder-Barboza, and J. De Koster. 2018. Symposium review: Modulating adipose tissue lipolysis and remodeling to improve immune function during the transition period and early lactation of dairy cows. *J. Dairy Sci.* 101:2737–2752. <https://doi.org/10.3168/jds.2017-13340>.
- Crookenden, M. A., A. Heiser, A. Murray, V. S. R. Dukkupati, J. K. Kay, J. J. Loor, S. Meier, M. D. Mitchell, K. M. Moyes, C. G. Walker, and J. R. Roche. 2016. Parturition in dairy cows temporarily alters the expression of genes in circulating neutrophils. *J. Dairy Sci.* 99:6470–6483. <https://doi.org/10.3168/jds.2015-10877>.
- Crookenden, M. A., K. M. Moyes, B. Kuhn-Sherlock, K. Lehnert, C. G. Walker, J. J. Loor, M. D. Mitchell, A. Murray, V. S. R. Dukkupati, M. Vailati-Riboni, A. Heiser, and J. R. Roche. 2019. Transcriptomic analysis of circulating neutrophils in metabolically stressed periparturient dairy cows. *J. Dairy Sci.* 102:7408–7420. <https://doi.org/10.3168/jds.2019-16367>.
- De Koster, J., M. Salavati, C. Grelet, M. A. Crowe, E. Matthews, R. O'Flaherty, G. Opsomer, L. Foldager, GplusE, and M. Hostens. 2019. Prediction of metabolic clusters in early-lactation dairy cows using models based on milk biomarkers. *J. Dairy Sci.* 102:2631–2644. <https://doi.org/10.3168/jds.2018-15533>.
- De Koster, J. D., and G. Opsomer. 2013. Insulin resistance in dairy cows. *Vet. Clin. North Am. Food Anim. Pract.* 29:299–322. <https://doi.org/10.1016/j.cvfa.2013.04.002>.
- Desdín-Micó, G., G. Soto-Herederó, and M. Mittelbrunn. 2018. Mitochondrial activity in T cells. *Mitochondrion* 41:51–57. <https://doi.org/10.1016/j.mito.2017.10.006>.
- Dimeloe, S., A. V. Burgener, J. Grählert, and C. Hess. 2017. T-cell metabolism governing activation, proliferation and differentiation; a modular view. *Immunology* 150:35–44. <https://doi.org/10.1111/imm.12655>.
- Diskin, M. G., J. J. Murphy, and J. M. Sreenan. 2006. Embryo survival in dairy cows managed under pastoral conditions. *Anim. Reprod. Sci.* 96:297–311. <https://doi.org/10.1016/j.anireprosci.2006.08.008>.
- Drackley, J. K., T. R. Overton, and G. N. Douglas. 2001. Adaptations of glucose and long-chain fatty acid metabolism in liver of dairy cows during the periparturient period. *J. Dairy Sci.* 84(Suppl.):E100–E112. [https://doi.org/10.3168/jds.S0022-0302\(01\)70204-4](https://doi.org/10.3168/jds.S0022-0302(01)70204-4).
- Duffield, T. 2000. Subclinical ketosis in lactating dairy cattle. *Vet. Clin. North Am. Food Anim. Pract.* 16:231–253. [https://doi.org/10.1016/S0749-0720\(15\)30103-1](https://doi.org/10.1016/S0749-0720(15)30103-1).
- Fenwick, M. A., R. Fitzpatrick, D. A. Kenny, M. G. Diskin, J. Patton, J. J. Murphy, and D. C. Wathes. 2008. Interrelationships between negative energy balance (NEB) and IGF regulation in liver of lactating dairy cows. *Domest. Anim. Endocrinol.* 34:31–44. <https://doi.org/10.1016/j.domaniend.2006.10.002>.
- Görgens, S. W., T. Benninghoff, K. Eckardt, C. Springer, A. Chadt, A. Melior, J. Wefers, A. Cramer, J. Jensen, K. I. Birkeland, C. A. Drevon, H. Al-Hasani, and J. Eckel. 2017. Hypoxia in combination with muscle contraction improves insulin action and glucose metabolism in human skeletal muscle via the HIF-1 α pathway. *Diabetes* 66:2800–2807. <https://doi.org/10.2337/db16-1488>.
- Grisart, B., W. Coppieters, F. Farnir, L. Karim, C. Ford, P. Berzi, N. Cambisano, M. Mni, S. Reid, P. Simon, R. Spelman, M. Georges, and R. Snell. 2002. Positional candidate cloning of a QTL in dairy cattle: identification of a missense mutation in the bovine DGAT1 gene with major effect on milk yield and composition. *Genome Res.* 12:222–231. <https://doi.org/10.1101/gr.224202>.
- Grygiel-Górniak, B. 2014. Peroxisome proliferator-activated receptors and their ligands: nutritional and clinical implications—A review. *Nutr. J.* 13:17. <https://doi.org/10.1186/1475-2891-13-17>.
- Ha, N. T., C. Drögemüller, C. Reimer, F. Schmitz-Hsu, R. M. Bruckmaier, H. Simianer, and J. J. Gross. 2017. Liver transcriptome analysis reveals important factors involved in the metabolic adaptation of the transition cow. *J. Dairy Sci.* 100:9311–9323. <https://doi.org/10.3168/jds.2016-12454>.
- Habel, J., and A. Sundrum. 2020. Mismatch of glucose allocation between different life functions in the transition period of dairy cows. *Animals (Basel)* 10:1028. <https://doi.org/10.3390/ani10061028>.
- Hammon, D. S., I. M. Evjen, T. R. Dhiman, J. P. Goff, and J. L. Walters. 2006. Neutrophil function and energy status in Holstein cows with uterine health disorders. *Vet. Immunol. Immunopathol.* 113:21–29. <https://doi.org/10.1016/j.vetimm.2006.03.022>.
- Hayirli, A., R. R. Grummer, E. V. Nordheim, and P. M. Crump. 2002. Animal and dietary factors affecting feed intake during the pre-fresh transition period in Holsteins. *J. Dairy Sci.* 85:3430–3443. [https://doi.org/10.3168/jds.S0022-0302\(02\)74431-7](https://doi.org/10.3168/jds.S0022-0302(02)74431-7).
- He, S., Q. Tong, D. K. Bishop, and Y. Zhang. 2013. Histone methyltransferase and histone methylation in inflammatory T-cell responses. *Immunotherapy* 5:989–1004. <https://doi.org/10.2217/imt.13.101>.
- Heimes, A., J. Brodhagen, R. Weikard, H.-M. Seyfert, D. Becker, M. Meyerholzer, W. Petzl, H. Zerbe, M. Hoedemaker, L. Rohmeier, H.-J. Schuberth, M. Schmicke, S. Engelmann, and C. Kühn. 2020. Hepatic transcriptome analysis identifies divergent pathogen-specific targeting-strategies to modulate the innate immune system in response to intramammary infection. *Front. Immunol.* 11:715. <https://doi.org/10.3389/fimmu.2020.00715>.
- Höfllich, A., H. Lahm, W. Blum, H. Kolb, and E. Wolf. 1998. Insulin-like growth factor-binding protein-2 inhibits proliferation of human embryonic kidney fibroblasts and of IGF-responsive colon carcinoma cell lines. *FEBS Lett.* 434:329–334. [https://doi.org/10.1016/S0014-5793\(98\)01011-4](https://doi.org/10.1016/S0014-5793(98)01011-4).
- Holcombe, S. J., L. Wisnieski, J. Gandy, B. Norby, and L. M. Sordillo. 2018. Reduced serum vitamin D concentrations in healthy early-lactation dairy cattle. *J. Dairy Sci.* 101:1488–1494. <https://doi.org/10.3168/jds.2017-13547>.
- Holness, M. J., and M. C. Sugden. 2003. Regulation of pyruvate dehydrogenase complex activity by reversible phosphorylation. *Biochem. Soc. Trans.* 31:1143–1151. <https://doi.org/10.1042/bst0311143>.
- Huang, W., B. T. Sherman, and R. A. Lempicki. 2009a. Bioinformatics enrichment tools: Paths toward the comprehensive functional analysis of large gene lists. *Nucleic Acids Res.* 37:1–13. <https://doi.org/10.1093/nar/gkn923>.
- Huang, W., B. T. Sherman, and R. A. Lempicki. 2009b. Systematic and integrative analysis of large gene lists using DAVID bioinformatics resources. *Nat. Protoc.* 4:44–57. <https://doi.org/10.1038/nprot.2008.211>.
- Ingvarsen, K. L. 2006. Feeding- and management-related diseases in the transition cow—Physiological adaptations around calving and strategies to reduce feeding-related diseases. *Anim. Feed Sci. Technol.* 126:175–213. <https://doi.org/10.1016/j.anifeedsci.2005.08.003>.

- Ingvarstsen, K. L., and J. B. Andersen. 2000. Integration of metabolism and intake regulation: a review focusing on periparturient animals. *J. Dairy Sci.* 83:1573–1597. [https://doi.org/10.3168/jds.S0022-0302\(00\)75029-6](https://doi.org/10.3168/jds.S0022-0302(00)75029-6).
- Ingvarstsen, K. L., R. J. Dewhurst, and N. C. Friggens. 2003. On the relationship between lactational performance and health: Is it yield or metabolic imbalance that cause production diseases in dairy cattle? A position paper. *Livest. Prod. Sci.* 83:277–308. [https://doi.org/10.1016/S0301-6226\(03\)00110-6](https://doi.org/10.1016/S0301-6226(03)00110-6).
- Ingvarstsen, K. L., and K. Moyes. 2013. Nutrition, immune function and health of dairy cattle. *Animal* 7(Suppl. 1):112–122. <https://doi.org/10.1017/S175173111200170X>.
- Kim, D., B. Langmead, and S. L. Salzberg. 2015. HISAT: A fast spliced aligner with low memory requirements. *Nat. Methods* 12:357–360. <https://doi.org/10.1038/nmeth.3317>.
- Kim, J. J., and D. D. Sears. 2010. TLR4 and insulin resistance. *Gastroenterol. Res. Pract.* 2010:212563. <https://doi.org/10.1155/2010/212563>.
- Kovrov, O., K. K. Kristensen, E. Larsson, M. Ploug, and G. Olivecrona. 2019. On the mechanism of angiotensin-like protein 8 for control of lipoprotein lipase activity. *J. Lipid Res.* 60:783–793. <https://doi.org/10.1194/jlr.M088807>.
- Krogh, M. A., M. Hostens, M. Salavati, C. Grelet, M. T. Sorensen, and D. C. Wathes. 2020. Between- and within-herd variation in blood and milk biomarkers in Holstein cows in early lactation. *Animal* 14:1067–1075. <https://doi.org/10.1017/S1751731119002659>.
- Li, H., B. Handsaker, A. Wysoker, T. Fennell, J. Ruan, N. Homer, G. Marth, G. Abecasis, R. Durbin, and 1000 Genome Project Data Processing Subgroup. 2009. The sequence alignment/map format and SAMtools. *Bioinformatics* 25:2078–2079. <https://doi.org/10.1093/bioinformatics/btp352>.
- Li, J., L. Li, D. Guo, S. Li, Y. Zeng, C. Liu, R. Fu, M. Huang, and W. Xie. 2020. Triglyceride metabolism and angiotensin-like proteins in lipoprotein lipase regulation. *Clin. Chim. Acta* 503:19–34. <https://doi.org/10.1016/j.cca.2019.12.029>.
- Li, X., S. Liu, X. Fang, C. He, and X. Hu. 2019. The mechanisms of DIRAS family members in tumor suppressor. *J. Cell. Physiol.* 234:5564–5577. <https://doi.org/10.1002/jcp.27376>.
- Loftus, R. M., and D. K. Finlay. 2016. Immunometabolism: Cellular metabolism turns immune regulator. *J. Biol. Chem.* 291:1–10. <https://doi.org/10.1074/jbc.R115.693903>.
- Loor, J. J., H. M. Dann, N. A. J. Guretzky, R. E. Everts, R. Oliveira, C. A. Green, N. B. Litherland, S. L. Rodriguez-Zas, H. A. Lewin, and J. K. Drackley. 2006. Plane of nutrition prepartum alters hepatic gene expression and function in dairy cows as assessed by longitudinal transcript and metabolic profiling. *Physiol. Genomics* 27:29–41. <https://doi.org/10.1152/physiolgenomics.00036.2006>.
- Lucy, M. C. 2001. Reproductive loss in high-producing dairy cattle: Where will it end? *J. Dairy Sci.* 84:1277–1293. [https://doi.org/10.3168/jds.S0022-0302\(01\)70158-0](https://doi.org/10.3168/jds.S0022-0302(01)70158-0).
- Lucy, M. C. 2008. Functional differences in the growth hormone and insulin-like growth factor axis in cattle and pigs: Implications for post-partum nutrition and reproduction. *Reprod. Domest. Anim.* 43:31–39. <https://doi.org/10.1111/j.1439-0531.2008.01140.x>.
- Lucy, M. C., G. A. Verkerk, B. E. Whyte, K. A. Macdonald, L. Burton, R. T. Cursons, J. R. Roche, and C. W. Holmes. 2009. Somatotrophic axis components and nutrient partitioning in genetically diverse dairy cows managed under different feed allowances in a pasture system. *J. Dairy Sci.* 92:526–539. <https://doi.org/10.3168/jds.2008-1421>.
- Lyons, N. A., J. S. Cooke, S. Wilson, S. C. van Winden, P. J. Gordon, and D. C. Wathes. 2014. Relationships between metabolite and IGF-1 concentrations with fertility and production outcomes following left abomasal displacement. *Vet. Rec.* 174:657. <https://doi.org/10.1136/vr.102119>.
- Mallard, B. A., J. C. Dekkers, M. J. Ireland, K. E. Leslie, S. Sharif, C. L. Vankampen, L. Wagter, and B. N. Wilkie. 1998. Alteration in immune responsiveness during the peripartum period and its ramification on dairy cow and calf health. *J. Dairy Sci.* 81:585–595. [https://doi.org/10.3168/jds.S0022-0302\(98\)75612-7](https://doi.org/10.3168/jds.S0022-0302(98)75612-7).
- Mamedova, L. K., K. Yuan, A. N. Laudick, S. D. Fleming, D. G. Mashek, and B. J. Bradford. 2013. Toll-like receptor 4 signaling is required for induction of gluconeogenic gene expression by palmitate in human hepatic carcinoma cells. *J. Nutr. Biochem.* 24:1499–1507. <https://doi.org/10.1016/j.jnutbio.2012.12.009>.
- Mann, S., A. S. Sipka, and J. K. Grenier. 2019. The degree of postpartum metabolic challenge in dairy cows is associated with peripheral blood mononuclear cell transcriptome changes of the innate immune system. *Dev. Comp. Immunol.* 93:28–36. <https://doi.org/10.1016/j.dci.2018.11.021>.
- Mantovani, A., C. Garlanda, A. Doni, and B. Bottazzi. 2008. Pentraxins in innate immunity: from C-reactive protein to the long pentraxin PTX3. *J. Clin. Immunol.* 28:1–13. <https://doi.org/10.1007/s10875-007-9126-7>.
- Mayasari, N., J. Chen, A. Ferrari, R. M. Bruckmaier, B. Kemp, H. K. Parmentier, A. T. M. van Kneegsel, and E. Trevisi. 2017. Effects of dry period length and dietary energy source on inflammatory biomarkers and oxidative stress in dairy cows. *J. Dairy Sci.* 100:4961–4975. <https://doi.org/10.3168/jds.2016-11857>.
- McCabe, M., S. Waters, D. Morris, D. Kenny, D. Lynn, and C. Creevey. 2012. RNA-seq analysis of differential gene expression in liver from lactating dairy cows divergent in negative energy balance. *BMC Genomics* 13:193. <https://doi.org/10.1186/1471-2164-13-193>.
- McCarthy, M. M., T. Yasui, M. J. Felipe, and T. R. Overton. 2016. Associations between the degree of early lactation inflammation and performance, metabolism, and immune function in dairy cows. *J. Dairy Sci.* 99:680–700. <https://doi.org/10.3168/jds.2015-9694>.
- McCarthy, S. D., S. M. Waters, D. A. Kenny, M. G. Diskin, R. Fitzpatrick, J. Patton, D. C. Wathes, and D. G. Morris. 2010. Negative energy balance and hepatic gene expression patterns in high-yielding dairy cows during the early postpartum period: A global approach. *Physiol. Genomics* 42A:188–199. <https://doi.org/10.1152/physiolgenomics.00118.2010>.
- Minuti, A., N. Jahan, V. Lopreiato, F. Piccioli-Cappelli, L. Bomba, S. Capomaccio, J. J. Loor, P. Ajmone-Marsan, and E. Trevisi. 2020. Evaluation of circulating leukocyte transcriptome and its relationship with immune function and blood markers in dairy cows during the transition period. *Funct. Integr. Genomics* 20:293–305. <https://doi.org/10.1007/s10142-019-00720-0>.
- Moyes, K. M., T. Larsen, and K. L. Ingvarstsen. 2013. Generation of an index for physiological imbalance and its use as a predictor of primary disease in dairy cows during early lactation. *J. Dairy Sci.* 96:2161–2170. <https://doi.org/10.3168/jds.2012-5646>.
- Nakagawa, Y., A. Satoh, H. Tezuka, S. I. Han, K. Takei, H. Iwasaki, S. Yatoh, N. Yahagi, H. Suzuki, Y. Iwasaki, H. Sone, T. Matsuzaka, N. Yamada, and H. Shimano. 2016. CREB3L3 controls fatty acid oxidation and ketogenesis in synergy with PPAR α . *Sci. Rep.* 6:39182. <https://doi.org/10.1038/srep39182>.
- Nakamura, M. T., B. E. Yudell, and J. J. Loor. 2014. Regulation of energy metabolism by long-chain fatty acids. *Prog. Lipid Res.* 53:124–144. <https://doi.org/10.1016/j.plipres.2013.12.001>.
- Nakano, M., Y. Suzuki, S. Haga, E. Yamauchi, D. Kim, K. Nishihara, K. Nakajima, T. Gotoh, S. Park, M. Baik, K. Katoh, and S. Roh. 2018. Downregulated angiotensin-like protein 8 production at calving related to changes in lipid metabolism in dairy cows. *J. Anim. Sci.* 96:2646–2658. <https://doi.org/10.1093/jas/sky162>.
- NRC. 2001. *Nutrient Requirements of Dairy Cattle*. Vol. 1. 7th ed. Natl. Acad. Press, Washington, DC.
- Osterloh, A., and M. Breloer. 2007. Heat shock proteins: Linking danger and pathogen recognition. *Med. Microbiol. Immunol. (Berl.)* 197:1–8. <https://doi.org/10.1007/s00430-007-0055-0>.
- Patel, S. B., G. A. Graf, and R. E. Temel. 2018. ABCG5 and ABCG8: More than a defense against xenosterols. *J. Lipid Res.* 59:1103–1113. <https://doi.org/10.1194/jlr.R084244>.
- Peng, J., and L. He. 2018. IRS posttranslational modifications in regulating insulin signaling. *J. Mol. Endocrinol.* 60:R1–R8. <https://doi.org/10.1530/JME-17-0151>.
- Pertea, M., G. M. Pertea, C. M. Antonescu, T.-C. Chang, J. T. Mendell, and S. L. Salzberg. 2015. StringTie enables improved reconstruction of a transcriptome from RNA-seq reads. *Nat. Biotechnol.* 33:290–295. <https://doi.org/10.1038/nbt.3122>.

- Puppel, K., and B. Kuczyńska. 2016. Metabolic profiles of cow's blood; a review. *J. Sci. Food Agric.* 96:4321–4328. <https://doi.org/10.1002/jsfa.7779>.
- Sadler, A. J., and B. R. Williams. 2008. Interferon-inducible antiviral effectors. *Nat. Rev. Immunol.* 8:559–568. <https://doi.org/10.1038/nri2314>.
- Salleh, M. S., G. Mazzoni, J. K. Höglund, D. W. Olijhoek, P. Lund, P. Lövendahl, and H. N. Kadarmideen. 2017. RNA-Seq transcriptomics and pathway analyses reveal potential regulatory genes and molecular mechanisms in high- and low-residual feed intake in Nordic dairy cattle. *BMC Genomics* 18:258. <https://doi.org/10.1186/s12864-017-3622-9>.
- Shahzad, K., M. Bionaz, E. Trevisi, G. Bertoni, S. L. Rodriguez-Zas, and J. J. Loo. 2014. Integrative analyses of hepatic differentially expressed genes and blood biomarkers during the periparturient period between dairy cows overfed or restricted-fed energy preparation. *PLoS One* 9:e99757. <https://doi.org/10.1371/journal.pone.0099757>.
- Sheldon, I. M., G. S. Lewis, S. LeBlanc, and R. O. Gilbert. 2006. Defining postpartum uterine disease in cattle. *Theriogenology* 65:1516–1530. <https://doi.org/10.1016/j.theriogenology.2005.08.021>.
- Shi, K., R. Li, Z. Xu, and Q. Zhang. 2020. Identification of crucial genetic factors, such as PPAR γ , that regulate the pathogenesis of fatty liver disease in dairy cows is imperative for the sustainable development of dairy industry. *Animals (Basel)* 10:639. <https://doi.org/10.3390/ani10040639>.
- Song, S., R. R. Attia, S. Connaughton, M. I. Niesen, G. C. Ness, M. B. Elam, R. T. Hori, G. A. Cook, and E. A. Park. 2010. Peroxisome proliferator activated receptor alpha (PPARalpha) and PPAR gamma coactivator (PGC-1alpha) induce carnitine palmitoyltransferase IA (CPT-1A) via independent gene elements. *Mol. Cell. Endocrinol.* 325:54–63. <https://doi.org/10.1016/j.mce.2010.05.019>.
- Su, W., Z. Mao, Y. Liu, X. Zhang, W. Zhang, J. A. Gustafsson, and Y. Guan. 2019. Role of HSD17B13 in the liver physiology and pathophysiology. *Mol. Cell. Endocrinol.* 489:119–125. <https://doi.org/10.1016/j.mce.2018.10.014>.
- Taylor, V. J., D. E. Beaver, and D. C. Wathes. 2003. Physiological adaptations to milk production that affect fertility in high yielding dairy cows. Pages 37–71 in *Dairying, using Science to Meet Consumer Needs*. Br. Soc. Anim. Sci. Occasional Pub. No. 29. E. Kebreab, J. Mills, D. Beaver, ed. Nottingham University Press, Nottingham, UK. <https://doi.org/10.1017/S0263967X00040040>.
- Taylor, V. J., Z. Cheng, P. G. A. Pushpakumara, D. C. Wathes, and D. E. Beaver. 2004. Relationships between the plasma concentrations of insulin-like growth factor-I in dairy cows and their fertility and milk yield. *Vet. Rec.* 155:583–588. <https://doi.org/10.1136/vr.155.19.583>.
- Tuckey, R. C., C. Y. S. Cheng, and A. T. Slominski. 2019. The serum vitamin D metabolome: What we know and what is still to discover. *J. Steroid Biochem. Mol. Biol.* 186:4–21. <https://doi.org/10.1016/j.jsbmb.2018.09.003>.
- Vangroenweghe, F., I. Lamote, and C. Burvenich. 2005. Physiology of the periparturient period and its relation to severity of clinical mastitis. *Domest. Anim. Endocrinol.* 29:283–293. <https://doi.org/10.1016/j.domaniend.2005.02.016>.
- Vernon, R. G. 2005. Lipid metabolism during lactation: A review of adipose tissue-liver interactions and the development of fatty liver. *J. Dairy Res.* 72:460–469. <https://doi.org/10.1017/S0022029905001299>.
- Viollet, B., M. Foretz, B. Guigas, S. Horman, R. Dentin, L. Bertrand, L. Hue, and F. Andreelli. 2006. Activation of AMP-activated protein kinase in the liver: A new strategy for the management of metabolic hepatic disorders. *J. Physiol.* 574:41–53. <https://doi.org/10.1113/jphysiol.2006.108506>.
- Vleurick, L., R. Renaville, M. VandeHaar, J. L. Hornick, L. Istasse, I. Parmentier, C. Bertozzi, C. Van Eenaeme, and D. Portetelle. 2000. A homologous radioimmunoassay for quantification of insulin-like growth factor-binding protein-2 in blood from cattle. *J. Dairy Sci.* 83:452–458. [https://doi.org/10.3168/jds.S0022-0302\(00\)74902-2](https://doi.org/10.3168/jds.S0022-0302(00)74902-2).
- Walesky, C., and U. Apte. 2015. Role of hepatocyte nuclear factor 4 α (HNF4 α) in cell proliferation and cancer. *Gene Expr.* 16:101–108. <https://doi.org/10.3727/105221615X14181438356292>.
- Walls, J., L. Sinclair, and D. Finlay. 2016. Nutrient sensing, signal transduction and immune responses. *Semin. Immunol.* 28:396–407. <https://doi.org/10.1016/j.smim.2016.09.001>.
- Wathes, D. C., Z. Cheng, N. Bourne, V. J. Taylor, M. P. Coffey, and S. Brotherstone. 2007b. Differences between primiparous and multiparous dairy cows in the inter-relationships between metabolic traits, milk yield and body condition score in the periparturient period. *Domest. Anim. Endocrinol.* 33:203–225. <https://doi.org/10.1016/j.domaniend.2006.05.004>.
- Wathes, D. C., Z. Cheng, W. Chowdhury, M. A. Fenwick, R. Fitzpatrick, D. C. Morris, J. Patton, and J. J. Murphy. 2009. Negative energy balance alters global gene expression and immune responses in the uterus of postpartum dairy cows. *Physiol. Genomics* 39:1–13. <https://doi.org/10.1152/physiolgenomics.00064.2009>.
- Wathes, D. C., A. M. Clempson, and G. E. Pollott. 2012. Associations between lipid metabolism and fertility in the dairy cow. *Reprod. Fertil. Dev.* 25:48–61. <https://doi.org/10.1071/RD12272>.
- Wathes, D. C., M. Fenwick, Z. Cheng, N. Bourne, S. Llewellyn, D. G. Morris, D. Kenny, J. Murphy, and R. Fitzpatrick. 2007a. Influence of negative energy balance on cyclicity and fertility in the high producing dairy cow. *Theriogenology* 68(Suppl. 1):S232–S241. <https://doi.org/10.1016/j.theriogenology.2007.04.006>.
- Weinberg, R. B., J. W. Gallagher, M. A. Fabritius, and G. S. Shelness. 2012. ApoA-IV modulates the secretory trafficking of apoB and the size of triglyceride-rich lipoproteins. *J. Lipid Res.* 53:736–743. <https://doi.org/10.1194/jlr.M019992>.
- Wu, J. W., H. Yang, S. P. Wang, K. G. Soni, C. Brunel-Guitton, and G. A. Mitchell. 2015. Inborn errors of cytoplasmic triglyceride metabolism. *J. Inher. Metab. Dis.* 38:85–98. <https://doi.org/10.1007/s10545-014-9767-7>.
- Zachut, M., H. Honig, S. Striem, Y. Zick, S. Boura-Halfon, and U. Moallem. 2013. Periparturient dairy cows do not exhibit hepatic insulin resistance, yet adipose-specific insulin resistance occurs in cows prone to high weight loss. *J. Dairy Sci.* 96:5656–5669. <https://doi.org/10.3168/jds.2012-6142>.
- Zerbe, H., N. Schneider, W. Leibold, T. Wensing, T. A. Kruip, and H. J. Schuberth. 2000. Altered functional and immunophenotypical properties of neutrophilic granulocytes in postpartum cows associated with fatty liver. *Theriogenology* 54:771–786. [https://doi.org/10.1016/S0093-691X\(00\)00389-7](https://doi.org/10.1016/S0093-691X(00)00389-7).
- Zhang, H., Q. Chen, T. Jiao, A. Cui, X. Sun, W. Fang, L. Xie, Y. Liu, F. Fang, and Y. Chang. 2014. Involvement of KLF11 in hepatic glucose metabolism in mice via suppressing of PEPCK-C expression. *PLoS One* 9:e89552. <https://doi.org/10.1371/journal.pone.0089552>.

ORCID

- D. C. Wathes  <https://orcid.org/0000-0002-8206-6091>
 Z. Cheng  <https://orcid.org/0000-0002-1559-5735>
 M. Salavati  <https://orcid.org/0000-0002-7349-2451>
 L. Buggiotti  <https://orcid.org/0000-0002-7404-7800>
 H. Takeda  <https://orcid.org/0000-0002-8455-6887>
 L. Tang  <https://orcid.org/0000-0001-9742-769X>
 K. I. Ingvarstsen  <https://orcid.org/0000-0003-2372-563X>
 C. Ferris  <https://orcid.org/0000-0001-8623-5983>
 M. A. Crowe  <https://orcid.org/0000-0003-1999-815X>